air, and even the discoloring effect of sunlight itself on the panel covering, as these factors can shorten system life and increase the cost of the energy produced. Designs that are candidates for large-scale use must be *capable of being manufactured economically in large quantities*. The *availability of materials* used in such cells must also be examined, along with all the *environmental impacts* associated with manufacture, use, and eventual disposal of these cells.

In this chapter we shall consider many of these characteristics as we discuss two types of cells—single-crystal Si cells and thin-film CdS/Cu_2S cells, operating in AM1 sunlight. We will here also consider the monetary and energy costs associated with various processes, such as those for purifying silicon. In Chaps. 9 and 10 we return to these topics while discussing less conventional fabrication processes and materials that appear promising for making low-cost cells for widespread terrestrial deployment.

The properties of a semiconductor such as silicon depend upon the processes used in its manufacture. Of greatest importance is the degree of crystalline perfection exhibited by the final product. In this section we shall briefly discuss this characteristic, and then turn to the processing techniques commonly used to form semiconductors and make them into functioning solar cells.

Table 4.1 lists properties of single-crystal silicon and cadmium sulfide. Although the electrical properties of these semiconductors are of primary interest, the other properties may be important in cell design. One must know the index of refraction in order to design a proper antireflection coating. Mechanical properties determine the stresses the cells can withstand when they are encapsulated, shipped, and installed. Thermal properties are important for concentrator cells. (Properties of many other semiconductors that are candidates for advanced cell designs are given in Chap. 10.)

We referred in Chap. 1 to solids having different degrees of crystalline perfection, as illustrated in Fig. 4.2. In a perfect single crystal, the arrangement of atoms around any one lattice point is repeated exactly at all other lattice points. Real crystals may approach such perfection. In a polycrystalline solid, long-range order of this sort exists *within* individual grains having diameters ranging from a fraction of a micron to millimeters. The term *semicrystal* used in Fig. 1.2 refers to polycrystalline materials with grain sizes at the very high end of this range. The grains are more or less randomly oriented with respect to each other, and thus where they meet the neighboring atoms do not "fit" correctly, resulting in local strains and distortions at the grain boundaries. In amorphous solids there is at most only short-range order that extends over just a few atoms at each location.

Until very recently silicon solar cells have been made from single-crystal material, to exploit its excellent electrical properties. The carrier mobilities

Table 4.1 Some Properties of Silicon and Crystalline Cadmium Sulfide

Property	Semiconductor	
	Si	CdS
Electrical		
Energy gap:		
E_g (eV)	1.12	2.6
Type	indirect	direct
Drift mobility:		
μ_n (cm^2/V·s)	1350	340
μ_p (cm^2/V·s)	480	50
Diffusion constant		
D_n (cm^2/s)	38	9
D_p (cm^2/s)	12	1.4
Intrinsic carrier concentration: n_i (cm^{-3})	1.6×10^{10}	
Relative dielectric permittivity (static) ϵ_r	11.7	8.9
Mechanical		
Crystal structure	cubic diamond	hexagonal
Density: ρ(kg/m^3)	2.238×10^3	4.82×10^3
Fracture strength (MN/m^2)	≈ 220	
(lb/in^2)	$\approx 31{,}000$	
Optical		
Index of refraction:	3.44	2.5
Thermal		
Thermal conductivity (W/cm·°C)	1.45	
Specific heat per unit volume (J/kg·°C)	7×10^{-4}	
Coefficient of linear thermal expansion (1/°C)	2.6×10^{-6}	
Melting point (°C)	1420	

are high, and there are no grain boundaries and few defects to act as sites for enhanced recombination of photo-generated electrons and holes. Recombination at defects reduces the minority-carrier lifetime and hence lowers the cell efficiency.

The minority-carrier lifetime is one of the most important electrical characteristics of the semiconductor in a solar cell, but it is not an intrinsic property of the semiconductor used. Rather, it can vary from one sample to another of a given semiconductor, and it can also change during the pro-

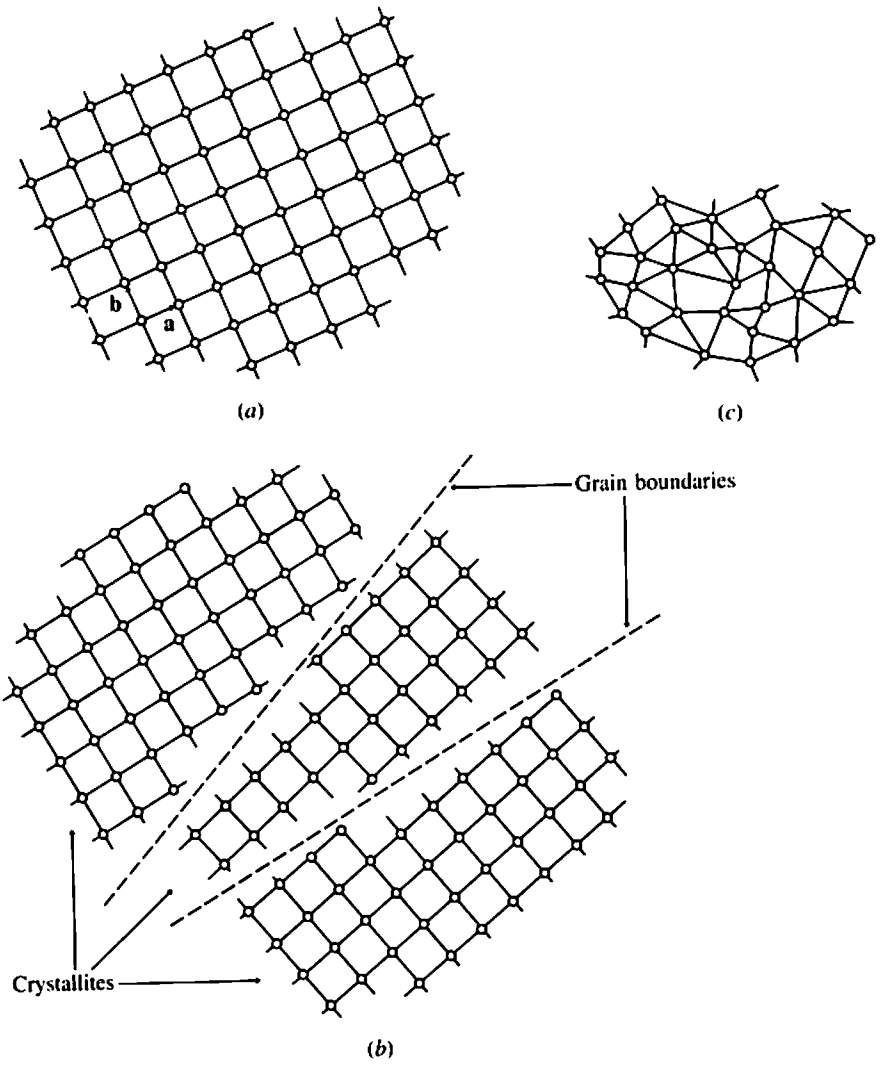

Figure 4.2 Portions of single-crystal, polycrystalline, and amorphous solids. (*a*) In a single crystal, atoms are regularly spaced throughout, and each atom can be reached from any other like atom by a translation that is the sum of integral multiples of primitive translation vectors such as **a** and **b**. (*b*) There is local order and translational symmetry in each crystallite of a polycrystalline solid, but the small crystallites may be differently oriented with respect to one another, meeting at their common borders to form grain boundaries. (*c*) There is no discernible local or long-range order in the amorphous solid, of which ordinary glass is the most familiar example.

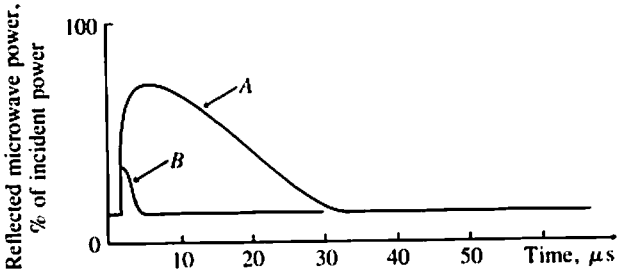

Figure 4.3 Oscilloscope displays of microwave power reflected by a silicon wafer when an intense flash of light creates electrons and holes that later recombine. Trace *A* is for an oxidized wafer, where recombination lifetime, indicated by the rate of decay of the pulse of reflected microwave power, is about 15–20 μs. Trace *B*, obtained with a bare, heavily ion-implanted silicon wafer, shows a very short lifetime.

cessing of a cell. This can be illustrated strikingly with the use of a microwave method to determine the lifetime.

In the microwave method, an oscilloscope displays the microwave energy reflected from a semiconductor wafer as a brief flash of light creates electron–hole pairs in the wafer. More microwave energy is reflected when wafer conductivity is high because of the light-produced carriers. As the carriers recombine, the conductivity and the microwave reflectivity fall. Figure 4.3 shows such a display of reflected microwave power from a carefully oxidized silicon wafer having a carrier lifetime around 15 or 20 μs (trace *A*). Trace *B* in Fig. 4.3 was made after ion implantation of the wafer—bombarding it with fast-moving ions, as described in the box in this chapter. The lifetime has decreased drastically because of the heavy damage caused by the impact of the high-energy ions near the surface of the wafer. This damage can be healed and the lifetime returned to nearly its initial value by heating the wafer in an inert atmosphere so that interstitial atoms can move into regular lattice sites. Similar reductions of lifetime occur when one etches away an oxide coating on a silicon wafer, or sandblasts the surface of a wafer, creating in both cases recombination centers at the surface at which electrons and holes can recombine.

This example shows how processing steps can affect material properties and hence cell performance. We now will consider the processes used to manufacture conventional silicon cells for terrestrial use.

4.2 CONVENTIONAL SILICON CELL PROCESSING

The four major steps in making silicon cells by presently conventional means are *forming crystals, doping, providing electrodes and an antireflection coat-*

ing, and *making a module* of interconnected cells, protected from chemical and physical attack from the atmosphere in which it is to operate.

Forming Single-Crystal Wafers

The objective is to produce large single-crystal wafers of Si three or more inches across, which have the following characteristics:

- Small number of defects per unit area.
- Controlled low concentrations of impurities (typically at some stage in the processing there will be only a few impurity atoms per billion host atoms of Si).
- Final thickness from 50 to 300 μm.
- Usually, one surface smooth enough for photolithography.

The conventional approach has been to purify the raw materials, grow single crystals by processes involving melting and slow solidification in carefully controlled temperature gradients, and then saw the resulting single-crystal ingot into slices that are polished as a final step. The chief contributors to cost and energy use in manufacture have been the purification and crystal-growth processes. Another costly feature of conventional processing is kerf loss—loss of up to a third of the single-crystal material in the form of "sawdust" produced when the ingots are cut into wafers. By way of a preview, note that processing improvements aimed at lowering costs (described in Chap. 9) are connected with improved methods of purification and ways of forming reasonably perfect crystals having nearly the final thickness and so not requiring wafering.

A typical conventional purification and crystal-growth process for making semiconductor grade silicon is summarized in Fig. 4.4. Quartzite pebbles—sand—are mixed with a source of carbon and reduced in a high-temperature electric-arc furnace to produce a relatively impure molten silicon, which is drained off and cooled rapidly in a boat, forming metallurgical-grade polycrystalline silicon (MG–Si). Reaction with HCl produces trichlorosilane gas, which is condensed and fractionally distilled to yield a much purer product indicated in Fig. 4.4 as semiconductor-grade (SeG) trichlorosilane. Reaction with hydrogen in a chamber containing a silicon substrate heated electrically to 1000 to 1200°C results in deposition of SeG–Si on the substrate.

To form single-crystal and still purer silicon, either the Czochralski (CZ) or the float-zone (FZ) solidification process is employed. In the CZ process, a small oriented piece of single-crystal silicon used as a seed is put in contact with the surface of the molten silicon in a crucible which is slowly rotated. Silicon from the melt freezes on the seed, which is slowly raised, resulting in the formation of a cylindrical single-crystal ingot from 3 to 5 inches in

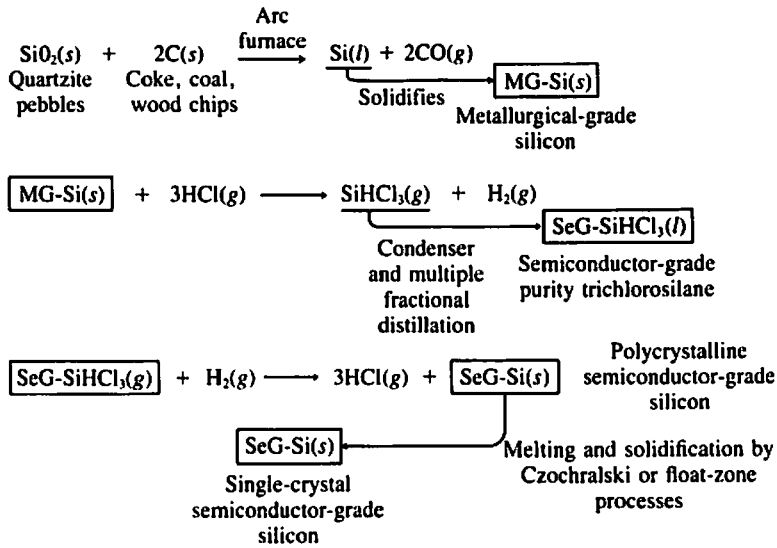

Figure 4.4 Conventional processes for making extremely pure, semiconductor-grade single-crystal silicon from sand. The symbols (*g*), (*l*), and (*s*) denote gaseous, liquid, and solid states, respectively.

diameter and up to 1 meter long. Some purification also occurs during CZ growth. In the float-zone method, a molten zone is passed through a relatively pure silicon ingot, causing a redistribution of impurities much as in the case of CZ growth. Because impurity concentrations in the liquid are generally higher than in the solid, passage of thin molten zones through an ingot having a 0.01 percent impurity content causes impurities to be swept to one end of the ingot, leaving in the middle a region having an impurity content as small as one part in 10^{10}. Finally, the cylindrical ingot is cut with saws into round wafers about 250 μm thick. Growth rates of only a few centimeters per hour are typical for CZ and FZ processes, and one goal of solar cell research and development is to find ways to make rapidly grown thin silicon sheets that do not require sawing.

Before following the wafers through the later steps of cell and array fabrication, let us consider the cost of this processing in terms of energy, money, and material. Many of the processing steps require volumes of material to be held at high temperature for many hours. This, together with the arc furnace reduction stage, requires a large energy input. At each stage of the processing, raw materials are lost. Of the silicon that is in the sand that enters the process, only about 20 percent emerges as SeG-Si, and about one-third of that is lost in the form of sawdust in the wafering step. Other materials are

lost during the processing as well. The starting materials cost only about \$0.21/kg, while the MG-Si is worth about \$84/kg (1980 dollars) because of the labor, energy, and supplies consumed and the equipment used in its production. The 1986 DOE goal of $\$0.70/W_{pk}$ cells can be reached with Si only if the cost of MG-Si can be lowered to about \$14/kg.

The dilemma of conventional processing for Si cells can also be expressed in terms of energy payback time. At each stage of cell manufacture, energy is expended in three forms:

1. Direct energy, such as the heat needed to liquify polycrystalline MG–Si for single-crystal growth.
2. Indirect energy used in the mining, transport, and manufacture of materials utilized, such as the HCl for the refinement stage.
3. Equipment and overhead energy embodied in the equipment used in the refining plant and energy expended in lighting, heating, and cooling the factory.

The individual and cumulative energy payback times for 12.5 percent efficient Si cells (Lindmayer et al., 1977) are shown in Fig. 4.5. The total payback time is 6.4 years, meaning that the cells would have to operate that long to produce energy equal to that used in their manufacture. The largest single components in this requirement are the direct energy used in Si refinement and the indirect energy used in panel building, accounting respectively for 2.6 and 1.0 years of the total. In Chap. 9 we shall describe an improved refinement process for which the energy payback time for reduction of sand to silicon and refinement together is reduced to only 0.85 years.

Doping

The objective is to create planar regions having different concentrations of impurities so as to form a *pn* junction. Thus in *n*-on-*p* Si cells, one may start with a *p*-type wafer containing boron as its chief impurity, and produce a very thin *n*-type layer near its surface by introducing phosphorus impurities into the wafer.

Impurities may be added intentionally to a molten semiconductor before solidification. The traditional method of forming a layer of different conductivity on the surface of such a wafer has been thermal diffusion of dopant atoms present in a gaseous molecule in a high temperature furnace in which the carefully cleaned wafers are placed as described in the box, Making an Integrated Circuit, earlier in this chapter.

Usually a two-step diffusion process is employed. In the *predeposition step* the desired impurity, transported by a carrier gas to the hot semiconductor surface, is diffused to a depth of a few tenths of a micron. For example,

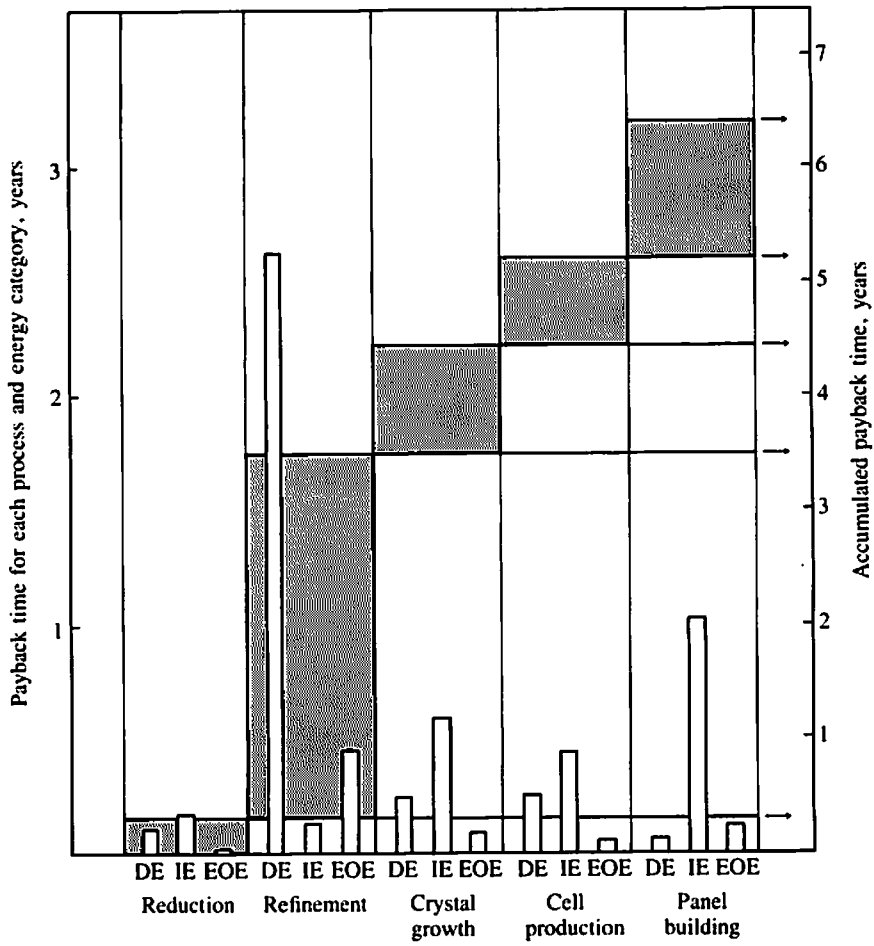

Figure 4.5 Energy payback times for fabricating 12.5-percent efficient AM1 silicon solar panels by conventional processes. Individual payback times for each stage, at left, and accumulated times, at right, are shown. Symbols: DE = direct energy; IE = indirect energy used in making materials expended in each stage; EOE = equipment and overhead energy. *(After Lindmayer et al., 1977).*

to dope Si with P, one may bubble nitrogen gas through liquid $POCl_3$ into a furnace held at from 800°C to 1100°C for anywhere from minutes to an hour or so. Alternatively, a solid oxide such as P_2O_5 might be heated for producing gaseous P_2O_5 which will react at the hot Si surface to form P and solid SiO_2. In the *drive-in step*, the semiconductor is simply heated and the predeposited dopant atoms diffuse into the semiconductor to a greater depth, up to about 1 μm.

Electrodes and Antireflection Coatings

In *pn*-junction solar cells, ohmic contacts are typically made with a uniform metallic electrode over the back surface and a fingerlike front electrode that permits light to pass between the opaque fingers. A transparent antireflection coating promotes transmission of light into the cell by reducing reflection, as discussed in Chap. 3. Some cells employ texturing of the semiconductor to reduce reflection.

Electrodes for conventional *pn*-junction cells must make ohmic contact to the underlying semiconductor; they should be highly conducting and should bond well by soldering to contact wires or conducting supports. Aluminum, gold, silver, and copper are conductive and solder well, but for ohmic contacting a heat treatment and additional metal layers between the metal and the semiconductor are often necessary. Furthermore, a metallic barrier layer may be needed to prevent diffusion of the electrode metal into the semiconductor where it might short-circuit the *pn* junction. As an example, an aluminum electrode deposited by evaporation onto the bare surface of a shallow-junction silicon *pn* diode requires a 5-minute heat treatment, typically at around 450°C, in forming gas (90 percent nitrogen, 10 percent hydrogen) or argon to make ohmic contact. During this treatment, aluminum might diffuse far enough in some regions to form conductive spikes that penetrate the junction, rendering the diode useless. To prevent this, one may deposit an Al–Si mixture with 5 percent Si instead, or evaporate a flash—a thin layer 100 to 200 Å thick—of a metal such as titanium or chromium which functions as a barrier to the aluminum that is evaporated over it.

For large-area flat-plate cells, electrodes may be deposited by any of several processes: evaporation of metal from an electrically heated filament or boat in a vacuum chamber, through an apertured mask; silk-screening onto the cell of a conductive paste such as an epoxy filled with metal powder with subsequent firing; and evaporation through a patterned layer made photolithographically in photoresist. This last process is used chiefly when the electrode pattern involves widths less than 100 μm, as may occur in concentrator cells. In such cells the currents are higher than in flat-plate array cells and electrode lines must be placed closer together on the cell to avoid large resistive losses. Once an electrode has been formed, it can be thickened by electroplating to reduce its series resistance.

As with veins in the leaf of a growing plant, which carry the products of photosynthesis away from individual cells (Fig. 4.6), the dimensions of the fingerlike front electrode on a solar cell are decided by an optimization process involving a compromise between reducing power losses due to series resistance and lowering the efficiency by making an overly dense, opaque electrode. Transparent conductive coatings may be used, as described further in Chap. 10. Cost and encapsulation considerations affect the thickness of the

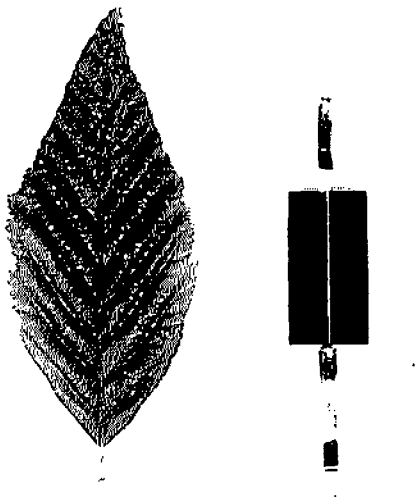

Figure 4.6 The pattern of bright fingerlike electrodes on a silicon solar cell is optimized to collect current efficiently without preventing much sunlight from reaching the underlying semiconductor. Note similarity with pattern of veins in leaf next to it.

electrode used. Simple calculation shows that a strip of aluminum 50 μm wide and 15,000 Å thick (bulk resistivity of Al is 2.7×10^{-6} Ω·cm) has a resistance of 3.6 Ω for each centimeter of length. Also important is the spacing between metal electrode strips. For 0.5-cm spacing, the diffused layer over the same 1-cm length of the cell would have a series resistance of 5 Ω. Reduction of the resistivity of the doped semiconductor layer between electrodes is only effective to a limited extent because doping that region too heavily has been found to degrade cell efficiencies (Sec. 3.7). Most commercial Si cells have electrodes roughly 50 μm thick, around 100 μm wide, and spaced by about 0.5 cm over the cell. Much finer, closely spaced electrodes are used on concentrator cells, illustrated in Chap. 7.

Just as with a coated camera lens, reflections are reduced by putting on antireflection (AR) coatings consisting of layers having indices of refraction between that of the semiconductor and the air. The simplest AR coating is a single layer whose thickness is one-quarter wavelength of light in the coating and whose index of refraction n_c is the geometrical mean of the indices of the two media contacting it, $n_c = (n_s)^{1/2}$, or 1.84 for Si. Though no material having exactly this index is known, some oxides and fluorides approximating it do exist (see Table 4.2). For example, over the whole usable solar spectrum, 90 percent of the light is transmitted through a 600-Å coating of Ta_2O_5 on Si.

Antireflection coatings are applied primarily by evaporation; the process can be continuous if the vacuum system has suitable pumped entrance and exit

Table 4.2 Indices of Refraction of Materials Usable as Anti-Reflection Coatings in Solar Cells
Indices are typical values for wavelengths near the middle of the solar spectrum

Material	Index of refraction
Al_2O_3	1.77
Glasses	1.5–1.7
MgO	1.74
SiO	1.5–1.6
SiO_2	1.46
Ta_2O_5	2.2
TiO_2	2.5–2.6

ports. Other means of coating include spraying, dipping, and spinning-on liquids that dry and are then heated to densify them.

The simple quarter-wavelength coating can be improved upon in several ways. With multiple layers, having the lowest index layer toward the sun, the reflection can be kept low over more of the solar spectrum than with the single layer. The presence of so-called native oxides (oxides that simply form in air at room temperature) on the semiconductor material of the cell itself may need to be taken into consideration in the coating design. Chemical means exist for texturing the semiconductor surface and even for producing a gradually varying index in a cover glass put over the cell to greatly improve transmission into the cell. The textured surface results when a single-crystal semiconductor is treated with an orientation-dependent etch that attacks some crystal planes faster than it does others. For example, etching a Si wafer whose normal orientation is in the (100) or equivalent direction in heated (90 to 95°C) hydrazine (36 percent N_2H_4) produces small pyramids whose faces are (111) planes (Fig. 4.7). Light incident on these pyramids is partially transmitted and partially reflected at each contact with their surfaces as the light bounces its way down toward the bottom of the pyramids. As with a properly designed AR coating, the surface of a textured cell appears dark when viewed in white light.

Fabricating Arrays

Objectives of the final steps are to connect individual cells electrically and mechanically, and to protect them from degradation due to thermal, chemical, and physical causes during use. Since about one-third of the final cost of a commercial cell is incurred in this stage, it is not surprising that automated array assembly is envisioned for low-cost cell fabrication.

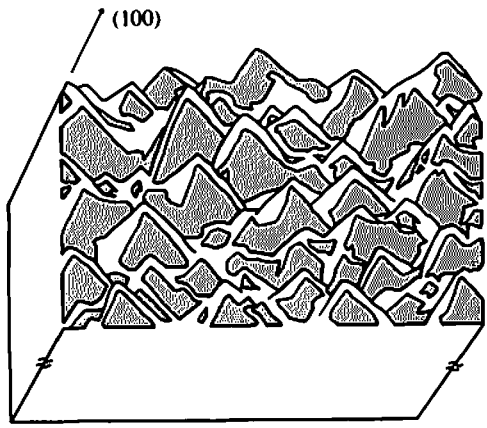

Figure 4.7 Textured surface of silicon that underwent orientation-dependent etching in hydrazine.

Conventionally, arrays have been made by electrically interconnecting individual cells, fastened to a plastic base, by wires or metal foil strips in a series-parallel arrangement. Finally, a glass or plastic sheet is fastened on the front in optical contact with the cells. Silicone-based potting compounds have been used to seal the cells for protection against degradation, particularly of their metallic electrodes, due to contact with moisture, salt, or reactive gases in the atmosphere.

Study of solar cell failures has shown that the encapsulant is responsible for many of the problems experienced. Failures have resulted from the separation of front covers from cells resulting in lowered cell efficiency because of the worsened optical contact between cover and cells, and from cracking of the encapsulant and subsequent penetration of moisture, and by discoloration of the covers. Best results usually are obtained with somewhat flexible panel assemblies which can adjust to strains produced during transport and installation of the array, and by temperature changes during actual use. Thus, potting compounds having a rubbery consistency tend to be favored, an example being silicone-based room-temperature-vulcanization (RTV) compounds, and resins that polymerize yet remain somewhat pliable. For protection against scratching due to abrasion in windstorms and sandstorms, glass has proven best. To avoid the discoloration noticed by desert travelers who find old bottles that have turned somewhat purple, glass with a low iron content is recommended. Among the plastics, polymethylmethacrylate has been found to retain its mechanical and optical properties well in 20-year exposure to actual AM1 sunlight in tests in the Arizona desert, whereas many other plastics weaken mechanically and discolor in just a few years in such light. The problem of concentrator cells is more difficult, because of the very

high light intensity and the need for removing excess heat from the cells (see Chap. 5). Solar simulators exist for carrying out accelerated life tests on cells and complete arrays, but more must be learned in this area since the cells themselves should last many decades *provided* they are protected from attack by the ambient atmosphere.

4.3 PROCESSING CADMIUM SULFIDE CELLS

Totally different processes are used for making polycrystalline thin-film CdS/Cu_2S cells. Forming single crystals is not required, and the emphasis is on inexpensive continuous methods for making large-area modules that, although less efficient than the single-crystal Si cells, are nevertheless economical.

The conventional CdS cell (Fig. 4.8) is made by evaporating a 25-μm-thick polycrystalline CdS layer onto a 25-μm-thick copper or molybdenum foil which serves as the back contact. The foil is then dipped briefly in CuCl solution at slightly below 100°C and Cu atoms replace Cd atoms at the surface to form an approximately 0.2-μm-thick Cu_2S layer. This layer accounts for the cell's response to photons from its bandgap, 1.1 eV and up. A contact grid of Cu or Au is evaporated or pressed on the top, and the cell is encapsulated with a plastic, such as a mylar sheet held in place with epoxy. Heat treatments may be used to improve cell photoresponse.

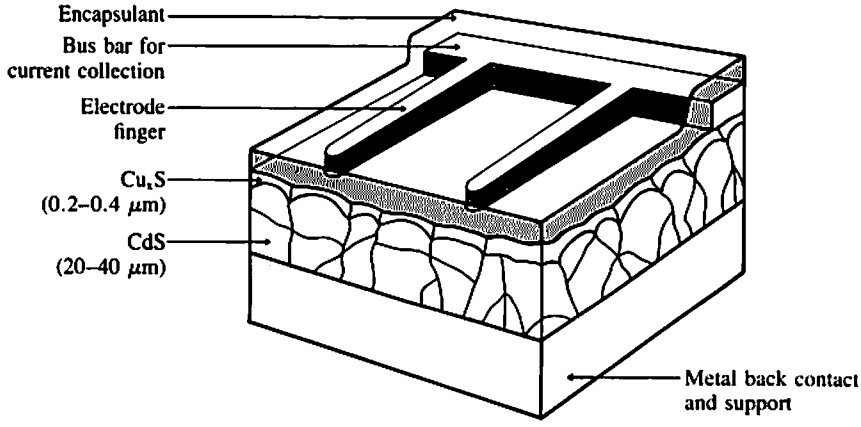

Figure 4.8 Cross-sectional view of polycrystalline cadmium sulfide (CdS/Cu_2S) solar cell.

A variety of other fabrication methods has been investigated, including use of a glass substrate coated with an optically transmitting and electrically conducting tin or indium oxide layer, and the use of spraying rather than evaporation to form the CdS layer (see Secs. 9.5 and 10.4).

Recombination at grain boundaries, leading to a lowering of the collection efficiency, and migration of Cu along grain boundaries into the cell, resulting in partial short-circuiting of the junction, are problems resulting directly from the polycrystalline structure of this cell. Additionally, the cells may suffer from oxidation of the Cu_2S to CuO and Cu_2O at temperatures above 60°C if air penetrates the encapsulation, and a light-activated change of Cu_2S to lower forms of Cu_xS has been identified as a problem in some of these cells.

Concerted work on the materials and the processing problems associated with these cells has resulted in steady increases in reported efficiencies and led to some optimism that such thin-film cells, having adequate operating lifetimes and possibly involving CdS with materials other than Cu_2S, will meet the 1986 cost goals (see Sec. 10.4).

4.4 ENVIRONMENTAL AND OTHER CONSIDERATIONS

So long as their costs are high, solar cells and photovoltaic (PV) systems will be used in very small quantities, and decisions about their design can be based strictly on technological grounds. As their costs fall and large numbers of PV systems are deployed, however, materials and processing techniques must be chosen only after careful consideration of additional factors—environmental impact, energy content of materials used in the systems, world supplies of the materials (discussed in Chap. 10), and the possible production rates that can be achieved in high-volume manufacture. One might add to this list, for less-developed countries, the possibility of local manufacture of cells and systems.

Environmental Effects

During normal operation, PV systems pose far fewer adverse environmental problems than do fossil-fueled or nuclear power plants. PV arrays do increase the absorption of solar energy locally and so could cause local changes of temperature and airflow, but no serious effects have been identified when large PV arrays have been simulated by areas of increased absorptance in computer models of global atmospheric behavior.

Some damage to plants, burrow-dwelling animals, and the fragile desert surface could occur as PV arrays are installed in desert regions. But more worrisome are two direct effects: (1) air contamination and possible human

health hazards due to emissions associated with the mining, transport, and processing of ores to form PV arrays, and (2) biological effects of ingesting or inhaling toxic substances released if cells are on a building that burns accidentally.

One way to express the probable impact of the former type of emissions is to compare those from a PV system with those from a conventional power plant. Studies have shown (OTA, 1978) that routine emissions of SO_2, NO_x, CO, hydrocarbons, particulates, and waste solids in the manufacture and use of concentrator PV systems having 20 years life would be produced in from only 3 months to about 2 years of (manufacture and) operation of a coal-burning power plant, with scrubbers, having the same rated power output. Corresponding figures for flat-plate PV systems range from $3\frac{1}{4}$ months to as much as 9 years, depending on the technology chosen. These figures indicate that PV systems in normal operation are indeed relatively benign.

Quite hazardous chemicals are used in the manufacture of semiconductor devices, examples being PH_3 and BCl_3 used as sources of impurity atoms of P and B in doping, and of HCl and carcinogenic organic chemicals in cleaning processes. Safe procedures for using such substances have been developed for the integrated circuits industry, but since the volumes used will be orders of magnitude larger in a fully developed solar cell industry, these emissions will have to be carefully controlled.

Concern for the toxicity of the semiconductors in PV systems themselves is based largely on accidental dispersal as a result of fire. There are no toxic effects directly associated with Si. Cadmium is a heavy metal posing serious health hazards for humans, yet anticorrosion coatings of cadmium have been used routinely for years. If GaAs cells were involved in a serious fire, toxic and carcinogenic arsenic compounds such as As_2O_3 might be released into the atmosphere, contaminating it and also perhaps nearby water supplies. That GaAs is expected to be used only in systems where the sunlight is concentrated by a lens or focusing mirror is a further worry, since the cells could vaporize if their cooling systems failed. The hazard of high temperatures in concentrator systems is offset, however, by the small quantity of semiconductor material present. One should also not ignore the hazards of concentrated sunlight to rooftops, if the tracking machinery should go awry, and to eyesight if even a small fraction of the concentrated beam is reflected into human eyes.

Energy Content of Materials Used

The concept of energy payback time, already mentioned in connection with the semiconductors in the cells, also applies to the choice of materials for PV system supports, tracking structures if any, antireflection coatings and encapsulants. As Table 4.3 shows, the equivalent thermal energy required for a unit

Table 4.3 Energy Consumption in Materials Processing
Ton used here, 2000 lb. Estimated uncertainty of entries, ±15% except order-of-magnitude entry for plastics is same as average for inorganic chemicals [*Makhijani and Lichtenberg (1971)*]

Material	Energy per unit of production, kWh_T/ton
Titanium (rolled)	140,000
Aluminum (rolled)	66,000
Copper (rolled or hard drawn)	20,000
Steel (rolled)	11,700
Zinc	13,800
Lead	12,000
Glass (finished plate)	6,700
Paper (finished, average)	5,900
Inorganic chemicals (averaged)	2,400
Plastics (order-of-magnitude, assumed same as inorganic chemicals)	2,400
Cement	2,200
Coal	40
Sand and gravel	18

of production varies greatly from material to material. To these figures must be added energy required for transportation, which is much smaller for locally produced materials such as sand, gravel, and cement than for materials such as steel and aluminum. When one includes energy for transportation over typical distances, along with energy lost in the depreciation of production machinery, the total energy expenditure per ton of cement is only 2300 kWh_T/ton, whereas that for aluminum reaches about 67,000 kWh_T/ton. (The subscript T denotes thermal energy, where 1 $kWh_T = \frac{1}{3}$ kWh of electrical energy.) The low energy required for production and use of cement, glass, and plastics suggests that they be used wherever possible in PV systems.

Production Rates

Once the design for a cost-effective, energy-efficient, and environmentally benign solar cell is found, the challenge is to manufacture it in sufficient quantities and fast enough so it can meet increasing demands for electricity. The extremely high rates of production of cells and optical coatings and encapsulants required can be appreciated from the following example.

> **Example:** Suppose that the consumption of electrical energy in the U.S. during the year 1980 was 2.2×10^{12} kWh, that the rate of consumption increased by 3 percent annually through the year 2000, and that we wish to meet 10 percent of the electricity demand in the year 2000 with 11 percent efficient solar cell systems. Assuming that the insolation is equal to that in El Paso, Texas (2000

kWh/m^2 per year), what area of cells would be required by the year 2000, and what would be the annual production rate in square meters if 5 percent of the total were to be manufactured each year?

$$\text{Area required} = \frac{(\text{total electrical energy in year 2000})(0.10)}{(\text{annual insolation/m}^2)(0.11)}$$

$$= \frac{(2.2 \times 10^{12})(1 + 0.03)^{20}\,(0.10)}{(2 \times 10^{3})(0.11)}$$

$$= 1.8 \times 10^{9}\ \text{m}^2 \text{ (or about 700 mi}^2\text{, an area about 26 miles on a side)}$$

$$\text{Area/year} = 1.8 \times 10^{9}/20 = 9 \times 10^{7}\ \text{m}^2\text{/yr (about 35 mi}^2\text{/yr)}$$

Thus it is necessary to produce about 35 mi^2 of arrays each year—an area that is 5.9 mi on a side. This production rate is also impressive when put in terms of the tons per year of materials required. A 2-μm-thick CdS film having a density of 4.8 g/cm^3 weighs about 20 tons per square mile, and a silicon wafer of standard thickness (0.010 in, or 250 μm) at 2.33 g/cm^3 weighs about 1170 tons per square mile. Thus a production of 35 mi^2 per year would amount to about 40,000 tons of silicon per year if wafers of standard thickness were used, an amount that is about 30 times the present annual U.S. production of semiconductor grade silicon. Clearly it is advantageous to use thin cells, and we must employ production processes capable of high rates if photovoltaic systems are to contribute significant amounts of energy.

Fortunately, some industrial plants are capable of the required high rates of production (Mattox, 1975). For example, an air-to-air strip coater exists that can coat a 150-cm-wide plastic sheet with 500 Å of aluminum at a speed of 60 m/min, resulting in a throughput of 5×10^7 m^2/year. Float-glass production in a single plant at a rate of 3×10^7 m^2 (10 mi^2) per year has been achieved. Both electron-beam evaporation and sputter-deposition coating of large glass panels are routine, high-rate industrial processes. Electrodeposition is a low-cost process that is also a candidate for high-volume production. For example, plants exist that electrodeposit 1-μm-thick tin layers on strip steel at rates of 500 m/min at a cost of a few cents per square foot, for an annual production of about 1.9×10^8 m^2. The rates quoted are applicable in principle to production of PV systems because these processes can be used to make antireflection coatings, contacts and, in the case of thin-film PV cells, the semiconductor layers themselves.

4.5 SUMMARY

Terrestrial solar cells have been made commercially of single-crystal silicon—because of its excellent electrical properties and well-developed

technology—and of thin-film CdS/Cu_2S—because of its low cost per unit area. To reduce the cost per watt of output, higher efficiency cell designs, and less energy-intensive and more automated processing is required. Adverse environmental impacts from silicon solar cell use are much less than for well-scrubbed coal-fired power plants. A number of industrial processes now used for other purposes exhibit production rates of the magnitudes required for significant solar cell and concentrator manufacture.

REFERENCES

Lindmayer, J., Wihl, M., and Scheinine, A. (1977), Energy Requirement for the Production of Silicon Solar Arrays, Report SX/111/3, Solarex Corp., Rockville, Md., October.

Makhijani, A. B., and Lichtenberg, A. J. (1971), An Assessment of Energy and Materials Utilization in the U.S.A., ERL-M310 (revised), Electronics Research Laboratory, University of California, Berkeley, September.

Mattox, D. M. (1975), Solar-Energy Materials Preparation Techniques, *J. Vac. Sci. Tech.*, Vol. 12, No. 5, 1023–1031, September.

OTA (1978), Application of Solar Technology to Today's Energy Needs, 2 vols., Office of Technology Assessment, Congress of the U.S. (June, September).

PROBLEMS

4.1 *Production of dopant required* For the production rate of silicon cells worked out in the Example in this chapter, determine the corresponding rate of production of phosphorus required to dope the thin front layer on the cells. Assume the front layer is doped n-type to about 10^{19} phosphorus atoms per cubic centimeter for a thickness of 1 μm, and determine the weight of phosphorus required per year. (The dopant is diffused in from the front surface of the silicon and distributed in a gaussian fashion, with a total number of dopant atoms per unit of cell area roughly equal to the value you will obtain assuming uniform distribution.)

4.2 *Need for flexible encapsulant* In use, a solar cell might experience ambient temperatures from -20 to $+40$°C or more. Find the change due to thermal expansion of the diameter of a 10-cm-diameter silicon solar cell and the 10-cm length of an aluminum mounting plate that might be used to support the cell (assume a thermal expansion coefficient of 24×10^{-6}/°C for aluminum and 2.6×10^{-6}/°C for silicon).

4.3 *Mineral supply for CdS cells* The weight ratio of Cd to S in CdS is 3.5:1, and the available supply of S is much larger than that of Cd. Using the same assumptions as in the Example in this chapter, find the peak watts that can be generated by CdS cells if all of the world production of Cd in one year, 2×10^4 metric tons, and if all of the identified Cd mineral resources in the world, 1×10^6 metric tons, are used to make CdS solar cells.

4.4 *Silicon material cost* Referring to Fig. 4.4, silicon costs about 10¢/kg in the form of quartzite ore, \$1/kg as MG–Si, \$80/kg as purified polycrystalline Si, \$250/kg as single crystal Si, and \$400/kg as wafers after 30 percent sawing loss. If the wafers are 0.025 cm thick and the specific weight of silicon is 2.33 g/cm^3, approximately how many peak watts can be generated by cells made from 1 kg of Si wafers? Use your intuition and arbitrary guesses to compare the potential savings in \$/W_{pk} as the results of a cheaper method of making MG–Si, (for example, one that reduces the cost of this step by half), of purifying Si or making solar cells from less pure Si, of growing crystal or cutting crystal into wafers, of making solar cells with polycrystalline Si, and of making 10-μm-thick (amorphous) Si solar cells. Try to be quantitative, though arbitrary. Many specific cost reduction methods will be discussed in Chaps. 9 and 10.

CHAPTER FIVE
CONCENTRATION OF SUNLIGHT

Technical and economic characteristics of optical concentrators and cells designed for use with them

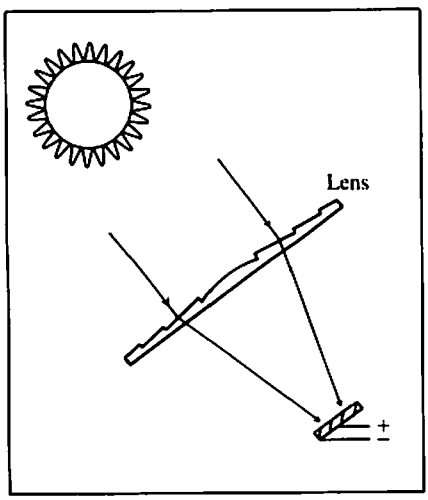

CHAPTER SIX
POWER CONDITIONING AND ENERGY STORAGE

Electronic systems for optimizing power output and overall usefulness of solar cells

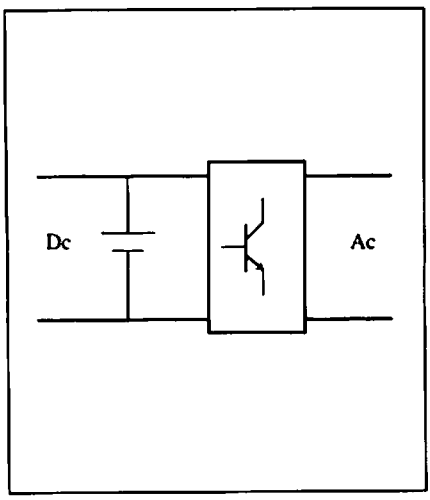

PART

TWO

CONCENTRATORS AND COMPLETE PHOTOVOLTAIC SYSTEMS

CHAPTER SEVEN
CHARACTERISTICS OF OPERATING CELLS AND SYSTEMS

Applications and operating characteristics of actual photovoltaic systems

CHAPTER EIGHT
ECONOMICS OF SOLAR CELL SYSTEMS

Cost analyses and other factors affecting solar cell use in industrialized and developing countries

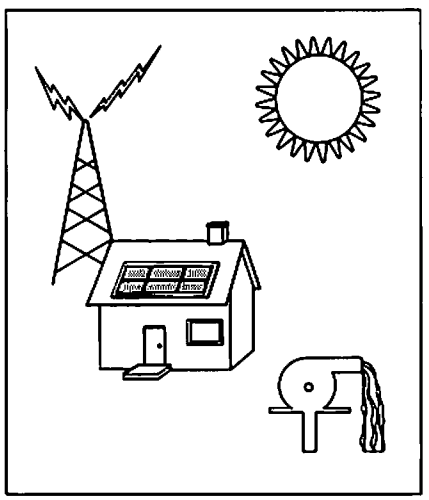

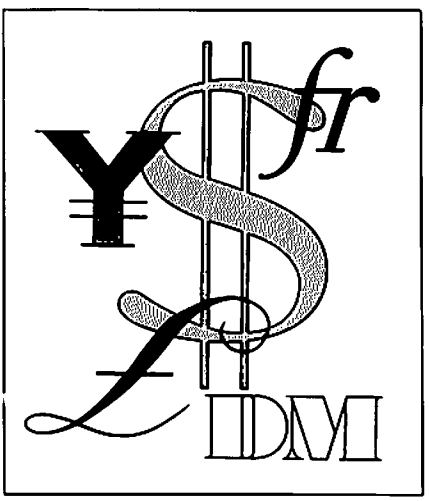

CHAPTER

FIVE

CONCENTRATION OF SUNLIGHT

CHAPTER OUTLINE

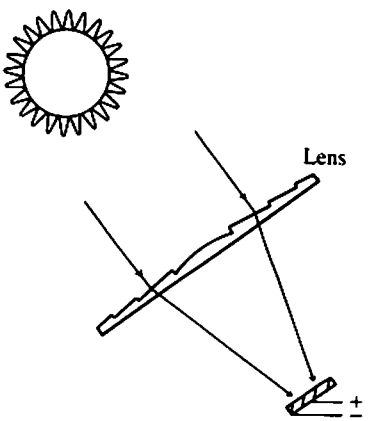

The intensity of solar radiation, about 1 kW/m^2 at noon on a clear summer day, the cost of each unit area of solar cells, and the cell efficiency together determine the minimum capital cost per watt of solar cell capacity. The cost of electricity generated from solar cells is high compared with that from conventional sources. One possible solution to the cost problem is to replace expensive solar cell area with low cost concentrator area and still derive about the same total power output. The economics of photovoltaic systems using sunlight concentration will be discussed in this chapter, with consideration of the relative cost advantage, the optical concentrators, and the need for tracking the sun.

A less obvious advantage of the concentrator photovoltaic system is that the conversion efficiencies of solar cells can be higher under concentrated sunlight. Furthermore, in a concentrator photovoltaic system, the cost of the solar cells is often only a small portion of the system cost, and relatively more extensive engineering efforts and costly cell manufacture technologies can be applied in order to bring about the high efficiencies. The reasons for the higher efficiencies and some other special considerations of concentrator solar cells will be presented.

5.1 SOLAR CONCENTRATORS

Sunlight concentration is not a new concept. In the history of solar energy applications (Meinel, 1977), particularly those that caught the public's attention, solar concentrators were used more often than not. Archimedes is said to have burned the invading Roman fleet of Marcellus in 212 B.C. by means of concentrated sunlight. Solar concentrators have been used to melt materials and to power heat engines. In the seventeenth century, lenses or burning glasses were the dominant form of concentrator. In the eighteenth and nineteenth centuries, the most popular concentrators were cone-shaped or parabolic reflectors. In the early twentieth century, many large solar energy projects used parabolic trough reflectors.

Today's concentrators for photovoltaic systems still have these basic forms. Bulk lenses, however, have been ruled out because of weight and cost, and are usually replaced by thin fresnel lenses to be described later.

Basic Concentrator Concepts

In evaluating a solar concentrator, the following are the key parameters to consider.

Concentration ratio If the collecting area of the lens or the reflector is 100 times the area of the solar cell, the concentration ratio of the system is said to be 100. The symbol "100×" is often used to denote this fact. The implicit

assumption is that the cell would be illuminated by light 100 times more intense than normal sunlight. In fact, the light intensity at the cell surface is almost certainly quite nonuniform because of the aberrations of the optical system. Furthermore, the average light intensity at the cell surface is likely to be less than 100 times the normal sunlight intensity because of the reflection, transmission, and scattering losses incurred along the paths of sun rays in the concentrator.

On the other hand, when a cell is said to have been tested under 100× AM1 illumination, the supposition is that it has been tested under uniform illumination equivalent to 100 times the intensity of AM1 sunlight.

Imaging and nonimaging concentrators If the solar cell is placed in the focal plane of a lens (or a reflector), as shown in Fig. 5.1*a*, the concentrator is said to be an *imaging* concentrator, as the sun's image is formed on the cell surface. Figure 5.1*b* shows a concentrator that does not form an image of the sun. Such concentrators are called *nonimaging* (Welford, 1978). The distinctions between imaging and nonimaging concentrators are often vague because many "imaging" concentrators are of such poor optical quality that they don't form any clear images and the solar cell may be placed away from the "focal plane."

One-dimensional and two-dimensional concentration A parabolic dish, for example, provides two-dimensional (2-D) concentration; a parabolic trough (see Fig. 5.2) provides one-dimensional (1-D) concentration.

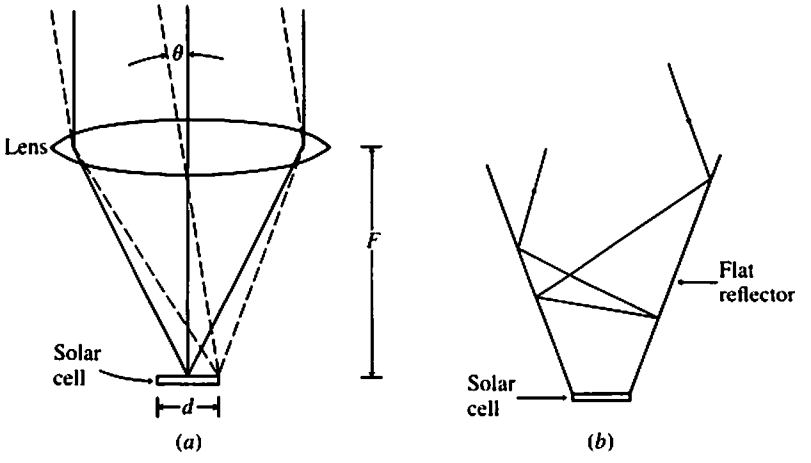

Figure 5.1 (*a*) Imaging concentrator. (*b*) Non-imaging concentrator. For either type, the acceptance angle decreases as the concentration ratio increases.

Acceptance angle In an imaging concentrator, as Fig. 5.1*a* shows, only rays incident within θ from the axis of the system can be focused on the solar cell. θ is called the *acceptance angle*. Lens (or reflector) optics shows (Born and Wolf, 1970)

$$d \approx 2F \sin \theta \tag{5.1.1}$$

The concentration ratio of the system is approximately D/d for 1-D concentration and $(D/d)^2$ for 2-D concentration. Therefore, the concentration ratio

$$C \approx \frac{1}{2f \sin \theta} \approx \frac{29}{f\theta} \qquad \text{1-D concentration} \tag{5.1.2}$$

$$C \approx \left(\frac{29}{f\theta}\right)^2 \qquad \text{2-D concentration} \tag{5.1.3}$$

where f, the f-number, is the ratio of the focal length F to the lens diameter D and $\sin \theta \approx \theta/58$ with θ in degrees. For a 2-D concentrator with $f = 1$ and $C = 100$, the acceptance angle is about 2.9°. Rays coming from outside this cone of acceptance will not be directed to the solar cell. It is difficult to manufacture concentrators with f much less than 1.

f-NUMBER OF A CAMERA LENS

Next to the lens of a camera there is an opaque screen, the aperture, with a round hole in the center. The diameter of the hole is adjustable and determines the effective diameter of the lens. For a given lens, the focal length F is fixed. Since the f-number is defined as

$$f\text{-number} = \frac{\text{focal length of lens}}{\text{effective diameter of lens}} = F/D$$

the f-number is inversely proportional to the diameter of the aperture. The amount of light entering the aperture is proportional to the area of the aperture, and thus to D^2 or $1/f^2$; therefore,

f-number	1.4	2	2.8	4	5.6	8	11
Relative amount of light entering aperture	1	1/2	1/4	1/8	1/16	1/32	1/64

This table explains the odd-looking f-numbers (e.g., 5.6) that one encounters and why photographers who want to expose film to the same amount of light energy, increase by a factor of two the length of time the shutter is open when they reduce the diameter of the aperture by one f-number (e.g., from $f2.8$ to $f4$).

For a nonimaging concentrator, Liouville's theorem (Born and Wolf, 1970) states that the 1-D concentration ratio is limited to

$$C \leq \frac{1}{\sin \theta} \approx \frac{58}{\theta} \tag{5.1.4}$$

Thus, there is an upper limit to concentration ratio for a given acceptance angle, and vice versa. Figure 5.1*b* illustrates the fact that rays coming outside the acceptance angle of a nonimaging concentrator may not reach the solar cell.

Solar tracking Earlier we saw the example of a 100× concentrator that has an acceptance angle of 2.9°. At the rate of motion of about 15° per hour (Chap. 2), the sun would sweep across the field of view of this concentrator (5.8°) in about 23 min. Clearly, a tracking mechanism will be needed to direct this concentrator toward the sun throughout the day. The tracking mechanism cannot be controlled precisely by a clock unless correction for the "Equation of Time" is provided (see Box). More interesting is the concept of automatic

THE EQUATION OF TIME

Sundials often include on them corrections (see photograph) for the small variations that occur through the year in the speed of the sun's apparent motion through the sky.

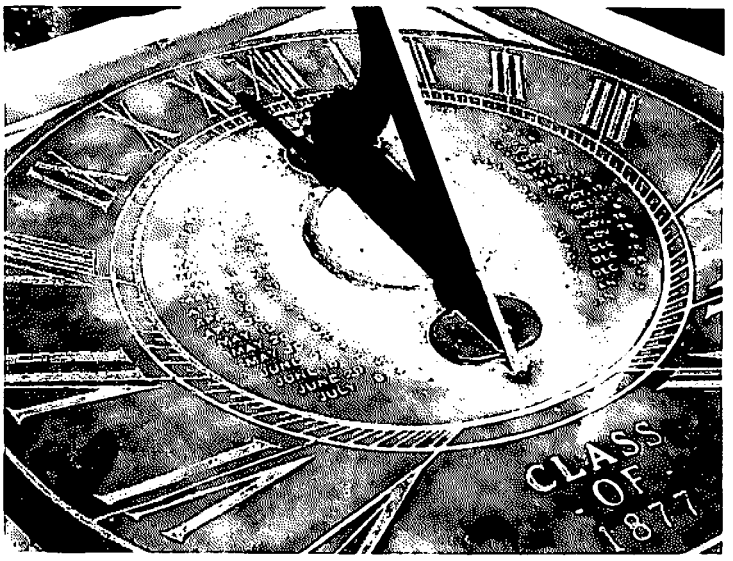

This sundial has stamped on it the number of minutes to be added to or subtracted from its indicated time on specific dates to correct for the varying speed of the sun's motion through the sky.

The average angular speed of the sun is 15° per hour. But if one observes the actual motion, one finds that the time of day at which the sun is at its highest point locally varies by as much as 25 min through the year. The so-called equation of time is defined as the time the mean sun, assumed moving at 15° per hour, is at the zenith minus the corresponding time for the actual sun.

The equation of time, plotted below as curve *C*, is composed of two main parts. One results from the variation of the earth's orbital speed owing to the change in earth-sun distance during the year. The earth's orbital speed is largest in January and smallest in June, causing the actual sun to arrive at its zenith earlier than expected during the first half of the year, and later in the second half (curve *A*). The second major effect arises from the tilt of the earth's axis. This correction is zero at the vernal and autumnal equinoxes, and at the summer and winter solstices. At other times of year, the tilt which causes the declination to change greatly also causes a small change in the time the sun is at the zenith (curve *B*).

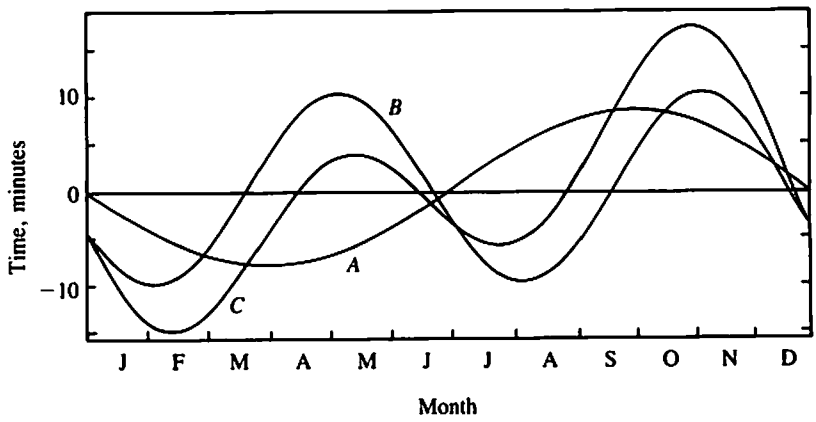

The correction given by the equation of time must be taken into account if one attempts to drive a tracking collector for solar cells by a clockwork mechanism.

solar tracking with the help of simple split-field photodiodes and electronics. To direct the concentrator during cloudy periods and to reset at the end of the day would probably require some artificial intelligence such as can be provided by a microprocessor. A few tracking mechanisms are commercially available (see Appendix 8). For some lower-concentration-ratio, one-dimensional concentrators, manual daily or even seasonal adjustments are satisfactory.

The highest possible concentration ratio in principle is set by the finite size of the solar disk, which requires an acceptance angle of 0.27° from the

concentrator. From Eq. (5.1.3), assuming $f = 1$, a 2-D concentration ratio of 11,500 would be possible. In reality, the imperfections of the optical components and the inaccuracies of the tracking mechanism would probably set a lower limit of about 1° to the acceptance angle. This in turn sets the upper limit of concentration ratio at about 1000.

Types of Solar Concentrators

We shall now examine the many different types of solar concentrators that have been considered for solar cell systems. Intensive development efforts have improved the optical efficiencies of concentrators to the 80 percent range, verified the expected economic advantage of concentrator systems, and narrowed the choices of concentrators. Boes (1980) has reviewed the solar cell concentrator system development programs in the United States and pointed out that the parabolic trough and the fresnel lens concentrators are by far the most popular types of concentrators. These programs tend to emphasize modules of a few-hundred-watt size with concentration ratios between 25 and 100. The upper limit of concentration ratio seems to be determined by the ready availability of suitable solar cells.

Parabolic troughs Parabolic troughs (Fig. 5.2*a*) are one-dimensional concentrators with single-axis tracking. The length of the trough lies in the north–south direction, either on a horizontal plane, or tilted toward the south (for northern hemisphere locations, as mentioned in Chap. 2). The tilt angle, furthermore, can be fixed or adjusted daily or seasonally.

The reflective materials are usually silvered glass, polished aluminum, or aluminized flexible film. The latter two materials are relatively cheap, but the reflectivity over the spectrum of interest is only about 85 percent with a sharp dip at 0.8 μm wavelength. The reflectance of silvered glass can be as high as 90 to 95 percent. The necessary curved shape can either be achieved by thermal sagging or mechanical bending.

A specific example of parabolic trough concentrators is the design used in the 240 kW photovoltaic demonstration project at Mississippi County Community College. Developed by Solar Kinetics, the concentrator measures 7 ft × 20 ft (2.1 m × 6.1 m) with the long axis aligned north–south horizontal. It has a concentration ratio of 42 and uses both aluminized film and silvered glass in different modules.

Another example is a General Electric design to be used in the 100 kW photovoltaic/thermal system at Sea World, Orlando, Florida. It measures 7 ft × 30 ft (2.1 m × 9.1 m) and has a concentration ratio of 34. The reflector is made of aluminized plastic film. The trough is mounted on a turntable with the long axis tilted. Changing the tilt angle and rotation of the turntable provides the tracking.

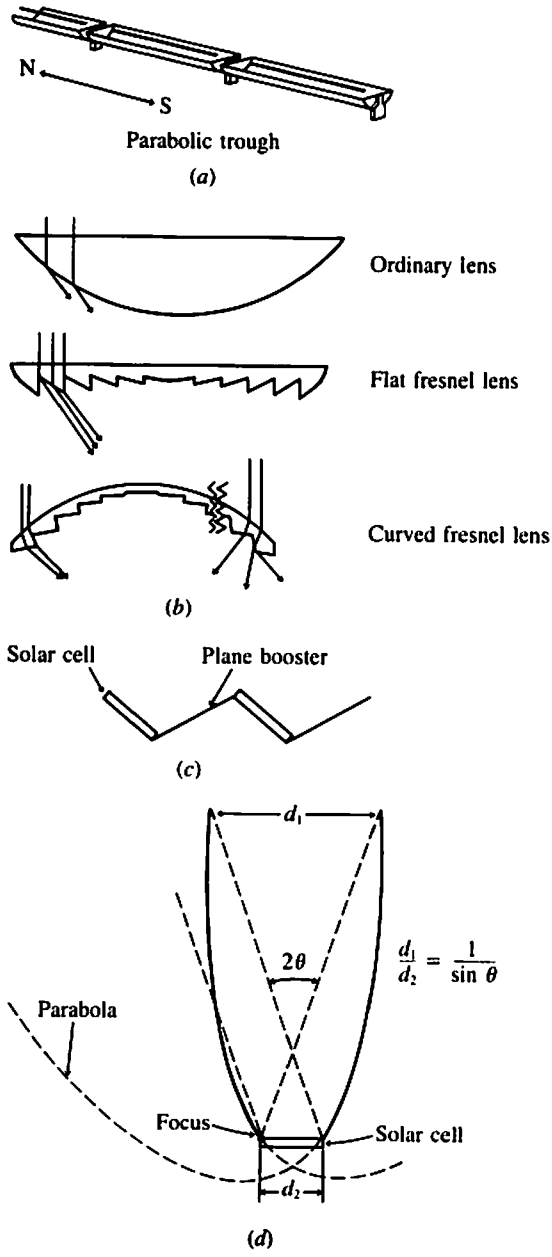

Figure 5.2 Types of concentrators: (*a*) parabolic trough, (*b*) fresnel lens, (*c*) plane booster, (*d*) compound parabolic concentrator, (*e*) parabolic dish, (*f*) central receiver concentrator, and (*g*) luminescent concentrator.

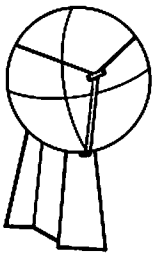

(*e*)

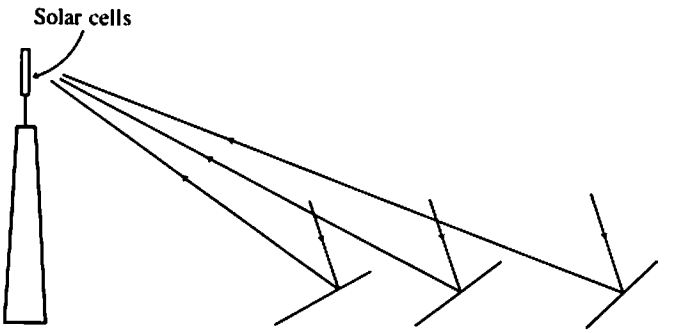

(*f*)

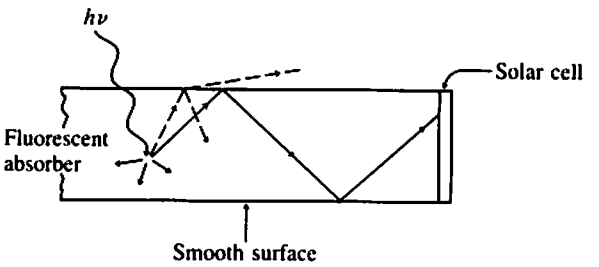

(*g*)

Figure 5.2 (*continued*)

Fresnel lens Figure 5.2*b* illustrates the derivation of the thin fresnel lens from a conventional lens. The sun rays are diffracted by a fresnel lens just as they would be by a conventional lens. The advantage of a fresnel lens is that it is much thinner and lighter than a conventional lens of the same diameter and f-number. Fresnel lenses are most often manufactured by injection molding of optical-quality plastic materials. It has been estimated that the sales

price of cast acrylic fresnel lens (Swedlow, 1976) in 1980 dollars would be about \$60/m^2 at a production rate of 15,000 m^2 per year. At 100,000 m^2 per year, the price would be \$42/m^2 for 0.635-cm-thick lenses and \$33/m^2 for 0.254-cm-thick lenses. It should be mentioned that thin fresnel *mirrors* may be made similarly with an added step of aluminizing.

Complex ray-tracing programs have been used to determine the size and shape of the fresnel lens grooves in order to reduce reflection loss and aberration and to achieve uniform illumination at the cell. James and Williams (1978) have shown that a curved (spherical or cylindrical) fresnel lens can further reduce reflection loss as well as enhance the mechanical rigidity. The facets in a curved lens should ideally be slanted inward to avoid reflection loss, as shown on the right-hand end of the lens in Fig. 5.2*b*. This, however, presents difficulty for the removal from the mold after injection molding. The first example described below presents a clever solution to this problem.

E-Systems has developed a concentrator whose arched fresnel lens is formed by simply bending a molded flat fresnel lens. It measures 3 ft × 8 ft (0.9 m × 2.4 m). The long axis runs north–south and is tilted toward the south. The tilt angle is adjusted daily while the single-axis tracking about the long axis is continuous. This concentrator is said to be capable of concentration ratios over 1000. In the 27-kW experiment at the Dallas Airport, this concentrator will operate at 25× concentration.

Another example worth noting is the fresnel concentrator system used in the very large 350-kW Soleras village electrical power project installed in Riyadh under joint support by the United States and Saudi Arabian governments. Designed by Martin Marietta, Inc., the basic unit is a flat 1 ft × 4 ft (0.31 m × 1.2 m) molded lens that contains four 1 ft × 1 ft (0.31 m × 0.31 m) lenses. Sixty-four such units (see Fig. 7.5) are mounted on a pedestal equipped for 2-D tracking. The concentration ratio is about 40.

Flat-plate concentrator The simplest form of a flat-plate concentrator or booster is shown in Fig. 5.2*c*. The solar cell output can be enhanced by about 50 percent (Hill, 1977). This type of concentrator has been proposed for use with the space-satellite photovoltaic generation station (Sec. 12.4).

Compound parabolic concentrator Winston (1974) proposed an elegant realization of Liouville's limit [Eq. (5.1.4)]. This concentrator, also known as a *Winston collector*, not only provides a large acceptance angle but also allows all sun rays within the acceptance angle to reach the solar cell after at most one reflection. As shown in Fig. 5.2*d*, the 1-D concentrator is formed with two parabolic cusps that satisfy these two conditions: (1) the focus of one cusp must be placed on the other, and (2) a line connecting the focus of one parabola to the top of its cusp must be parallel to the axis of the other parabola. With these facts in mind it is easy to see that $d_2/d_1 = \sin \theta$

(Liouville's theorem) and that a sun ray within the acceptance angle θ reaches the solar cell after at most a single reflection.

Because of its rather large acceptance angle, this collector is used primarily as a nontracking concentrator with the length of the trough running east–west. At solstices, the sun stays within the acceptance angle of a 5× concentrator for up to 8.7 hours, and a 10× concentrator for 6.8 hours (Meinel, 1976).

The disadvantage of the compound parabolic concentrator is that it requires a large area of reflective surface in comparison with other concentrators. The upper portion of a full Winston collector, however, can be arbitrarily trimmed, resulting in a much shorter structure with only slightly reduced concentration ratio. The resultant structure is called a *truncated* Winston collector. A 2-D Winston collector can be generated by making a surface of revolution from the cross-section of the 1-D concentrator.

Parabolic dish As shown in Fig. 5.2*e*, parabolic dishes require two-axis tracking and provide very high concentration ratios.

Central receiver concentrator As shown in Fig. 5.2*f*, the total mirror-surface area in one module can collect from tens of kilowatts to tens of megawatts. This has lately been the preferred concentrator for solar-thermal-electricity generation but has never been seriously discussed for concentrator photovoltaic systems.

Luminescent concentrator As shown in Fig. 5.2*g*, this unusual concentrator is made of a liquid or solid plate containing fluorescent materials, such as an organic dye or Nd ions. Sunlight is absorbed by the fluorescent material, which re-emits light semi-isotropically. A good portion of the re-emitted light is trapped in the plate by total internal reflection until it reaches the edge of the plate where it is absorbed by the solar cell.

A severe limitation of this potentially inexpensive, nontracking concentrator is its low optical efficiency. At low concentrations of the fluorescent material, absorption of sunlight is far from complete, whereas high concentrations would cause a photon to go through multiple absorption/emission cycles before reaching the solar cell with less than unity quantum efficiency at each cycle. Many ingenious improvements have been suggested over the recent years (Rapp, 1978) but the optical efficiency is still only about 20 percent.

Holographic concentrator A hologram is basically a large diffraction grating that modifies the wavefronts of light waves in a predetermined and usually complex way. Its ability to form three-dimensional images is well known. A hologram can also perform simpler tasks such as diffracting or

focusing a light beam. Since a hologram's operation is based on diffraction and is thus sensitive to the wavelength, a holographic concentrator cannot collect sunlight over the entire solar spectrum unless multiple holograms are used. The wavelength sensitivity, on the other hand, can be exploited for spectrum-splitting systems (see Chap. 12, Sec. 12.1). By using multiple holograms, the need for solar tracking can be eliminated (Ludman, 1982). Holographic concentrators are more expensive than fresnel lenses and their ability to stand long-term UV exposure is questionable.

5.2 ECONOMICS OF CONCENTRATOR PHOTOVOLTAIC SYSTEMS

As stated at the beginning of this chapter, the per-unit-area cost of solar cells seems to be the largest and most variable cost item in a photovoltaic system. We shall now compare the maximum acceptable unit-area cell costs of a flat-plate and a concentrator system. The cost of electricity generated by solar cells can be estimated from the following equation:

$$\text{Cost/kWh} = \frac{\text{cost of plant} \cdot \text{amortization rate}}{\text{kWh produced each year}} + \text{operating cost} \qquad (5.2.1)$$

For a relative comparison, we shall use the following numbers, which are believed to be reasonable.

Acceptable cost per kWh: \$0.06
Cost of plant excluding cells
  Direct: \$170 per peak kW for power conditioning, buildings, and battery storage for half day, and \$30/m^2 for flat-plate system for land, support structure, etc., or \$70/m^2 for concentrator system for land, concentrator, tracking structure, etc.
  Indirect: 40 percent of direct cost for architect and engineer fees, interest during construction, etc.
Amortization rate: 12 percent for interest and principal payments
Solar insolation: 4.4 kWh/day/m^2 (Chap. 2)
Operating cost: \$0.005/kWh

Let C be the maximum acceptable cell cost (\$/m^2), X the concentration ratio, and η the cell conversion efficiency. Considering 1 m^2 of collection area, Eq. (5.3.1) becomes

$$0.06 = \frac{C + 30 + 170 \cdot \eta}{4.4 \cdot 365 \cdot \eta} \cdot 1.4 \cdot 0.12 + 0.005 \qquad (5.2.2)$$

for a flat-plate system, or

$$0.06 = \frac{C/X + 70 + 170 \cdot \eta}{4.4 \cdot 365 \cdot \eta} \cdot 1.4 \cdot 0.12 + 0.005 \qquad (5.2.3)$$

for a concentrator system. The maximum acceptable costs per m^2 of cells are listed in Table 5.1. The table leads to several interesting conclusions:

1. Even if cells cost nothing, they must have some minimum efficiencies (8.4 percent for flat-plate, 19.6 percent for concentrator systems).
2. There is much greater incentive to strive for high cell efficiencies in concentrator systems than in flat-plate systems.
3. Very high manufacturing costs can be tolerated for high efficiency, high concentration-ratio cells.

The numbers in Table 5.1 are of course sensitive to the assumptions made for plant costs, but the qualitative conclusions listed above are not. DeMeo (1978), for example, concluded that future large-scale photovoltaic power plants will likely use either very low-cost flat-plate systems or very high-efficiency concentrator systems. In Chaps. 11 and 12, some exotic and expensive concentrator cells and systems will be described; their development is justified by the preceding economic analysis. One may get some additional feeling for the relative costs of concentrator and flat-plate systems from the following figures. Eight manufacturers made independent projections for the cost of concentrator arrays (concentrators, cells, and tracking systems) in 1976 dollars (Maycock, 1978) for an assumed production rate of 10 MW/year. The projections ranged between \$1.59 and \$2.31 per peak watt. These prices were several times lower than the flat-plate array costs.

One must not leave this subject without two sobering throughts. First, although concentrator systems can accept very high cell costs, providing cells at costs lower than the acceptable maximum would cause little reduction in the cost of the electricity generated. Second, the unit-area cost of concentrators appears to have less potential for significant reduction through technological innovations than the area cost of solar cells. In the long run, the

Table 5.1 Maximum acceptable cell cost per m^2

η		8.4%	10%	15%	19.6%	25%	30%
Flat-plate		\$0	\$5.5	\$23	\$40	\$59	\$76.5
Concentrator	$X = 10$	\$0.06/kWh goal cannot			\$0	\$187	\$365
	$X = 100$	be attained with any cell			\$0	\$1870	\$3650
	$X = 1000$	cost if $\eta < 19.6\%$			\$0	\$18,700	\$36,500

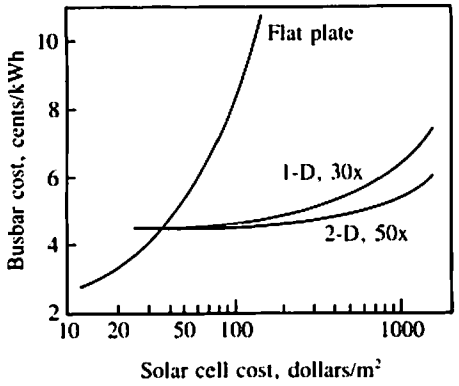

Figure 5.3 Cost of electricity as a function of per-unit area cost of solar cells.

flat-plate systems may yet prove to be the more economical. These conclusions can be easily evaluated using Eq. (5.2.1). Hovel (1978) presented a similar analysis, whose results are shown in Fig. 5.3.

5.3 CONCENTRATOR SOLAR CELLS

The structures and theory of concentrator solar cells are basically no different from those of nonconcentrator cells discussed in Chap. 3. To be sure, there are some subtle differences in the theory, but we shall ignore them for simplicity (Fossum, 1978). Figure 5.4*a* shows the measured and extrapolated J_{sc}, V_{oc}, and η of a small Si solar cell at constant temperature. J_{sc} is seen to increase in proportion to the concentration ratio, implying a constant collection efficiency. Because of increased J_{sc}, V_{oc} [Eq. (3.7.2)] also increases with increasing concentration. The slope of the V_{oc} curve decreases at high concentrations due to the high-level injection effect and can be improved by using a back-surface field cell (Hu, 1978). Figure 3.16 shows that the fill factor also increases with increasing J_{sc}. Therefore, the conversion efficiency η rises with increasing concentration ratio.

Large area cells typically show a peak in efficiency as seen in Fig. 5.4*b*. At high concentrations, the cell current is large and a considerable voltage is lost due to the series resistance in the cell (Sec. 3.8). Depending on the value of the cell series resistance, the efficiency would peak at different concentration ratios. By using a closely spaced, fine metal grid for the front contact, RCA (O'Donnell, 1978) has developed a Si solar cell whose efficiency peaks at about 18 percent at 300× concentration. Figure 5.4*c* shows the calculated efficiency for a GaAs cell with the series resistance as a parameter.

Several novel cell structures to be described in Chap. 11 have exceedingly small series resistance and can operate at up to 1000× concentration.

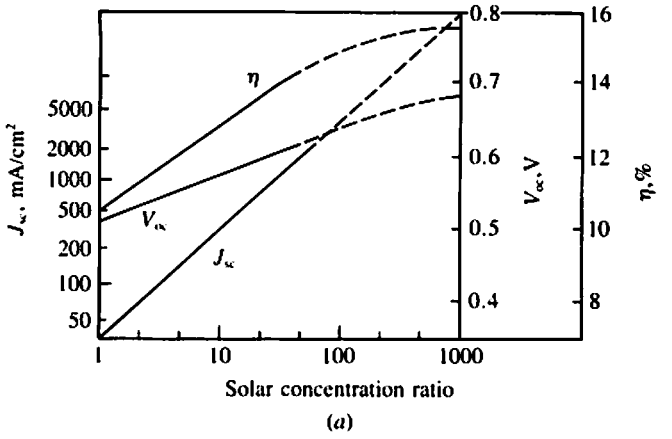

(*a*)

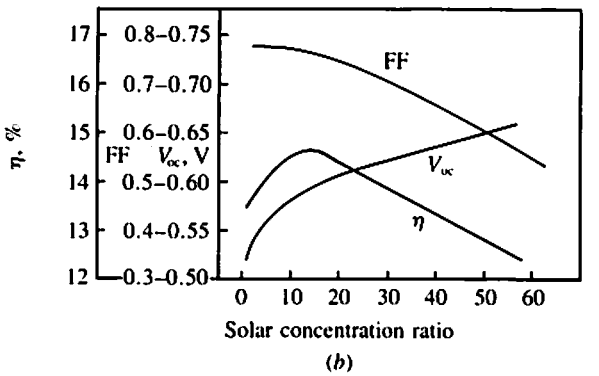

(*b*)

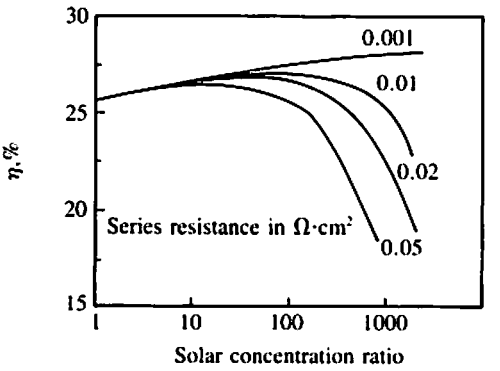

(*c*)

Figure 5.4 Conversion efficiency as a function of concentration ratio. (*a*) A small test solar cell with minimal series resistance; measurements and extrapolations. (*b*) A typical large-area solar cell. (*c*) Calculated efficiency of a GaAs cell.

5.4 COOLING AND COLLECTION OF THERMAL ENERGY

Solar concentration necessarily raises the temperature of the cell. Passive or active cooling must be provided in order to retain the high cell efficiency. This adds to the cost of the system. On the other hand, thermal energy becomes a by-product of concentrator photovoltaic systems. This may increase the economic values of the systems.

The temperature of the cell is determined by the thermal power influx and the thermal resistance of the heat path R_θ by

$$T_c \approx T_a + 1(\text{kW/m}^2) \cdot X \cdot \text{cell area (m}^2) \cdot (1 - \eta) \cdot R_\theta(\text{°C/kW}) \tag{5.4.1}$$

where T_c is the cell temperature, T_a is the temperature of the ambient air or liquid coolant, X is the concentration ratio, and η is the cell efficiency. Increasing X causes T_c to rise. With increasing cell temperature, I_{sc} tends to rise due to improved carrier lifetimes but the fill factor and the open-circuit voltage decrease. The temperature dependence of V_{oc} was discussed in Sec. 3.8. The net effect is that the silicon cells' efficiencies follow

$$\eta(T_c) \approx \eta(25\text{°C}) \cdot [1 - 0.004(T_c - 25)] \tag{5.4.2}$$

Clearly, minimizing T_c would maximize η but would also maximize the heat-exchanger cost.

Edenburn (1980) has made a comprehensive study of the optimization of heat exchanger designs. His basic conclusions are:

1. Passive cooling is effective and more economical than active cooling for 2-D concentrators (point focus) having lens sizes smaller than 0.1 m^2. Cooling effectiveness depends on the lens size but is quite insensitive to the concentration ratio because the available heat-exchanger-to-air interface area is determined by the lens size. For example, at a wind speed of 3 m/s, the cell temperature can be T_a + 73°C at X = 170 and T_a + 85°C at X = 3400. The cost of the optimal heat exchanger would be about \$10 for each m^2 of lens size in 1980 dollars.
2. Active cooling is preferred for 2-D concentrators with lens areas much larger than 0.1 m^2 and for 1-D concentrators (line focus). The equipment cost is about \$8 per m^2 of collector area and the energy use is about 7 percent of the cell output.

Edenburn's study suggested that an optimal system may have T_c as high as 80 to 100°C. At this temperature, the thermal energy may be collected and used rather efficiently for space heating or water heating. Where the thermal energy can be used readily, as is the case with the concentrator photovoltaic systems installed on or near residences or other buildings, studies have shown

that the total thermal energy produced by the system has about the same value as the electricity (Boes, 1980).

GaAs cells lose their efficiencies with increasing T at about half the rate of Si cells (Sec. 3.8). Therefore they can be operated at higher temperatures. This tends to reduce the heat-exchanger cost and allows GaAs solar cell systems to provide thermal energy at higher temperatures for industrial process heat or for driving thermal engines. For example a 1000× GaAs system employing passive cooling and having 18 percent module efficiency has been reported (Kaminar et al., 1982). In it the junction temperature is 50°C when the ambient temperature is 28°C.

5.5 SUMMARY

Concentrator solar cell systems trade the added costs of the optical concentrators for the costs of solar cells. There are many types of concentrators, but the fresnel lens and the parabolic trough reflector have received the most attention for use in photovoltaic systems. Since a concentrator system uses a much smaller quantity of solar cells than a flat-plate system of the same capacity, relatively more extensive engineering efforts and expensive manufacturing technologies can be applied to improving the efficiencies of concentrator solar cells. Further, a solar cell's efficiency increases with increasing light intensity until the series resistance of the cell causes this trend to be reversed. Many cell designs that minimize the effects of the series resistance are discussed in Chap. 11. Adequate means of cooling must be provided for concentrator solar cells. In some cases, the total thermal energy collected from a concentrator solar cell system has about the same commercial value as the total electricity generated by that system.

REFERENCES

Boes, E. C. (1980), Record, 14th IEEE Photovoltaic Spec. Conf., 994.
Born and Wolf (1970), *Principles of Optics*, Academic Press.
DeMeo, E. A., and Bos, P. B. (1978), Elec. Power Res. Inst. Report ER-589-SR.
Edenburn, M. W. (1980), Record, 14th IEEE Photovoltaic Spec. Conf., 771.
Fossum, J. G., Burgess, E. L., and Lindholm, F. A. (1978), *Solid-State Elec.*, Vol. 21, 729.
Hill, J. M., and Perry, E. H. (1977), Proc. 1977 Annual Meeting American Sec. of Inter'l Solar Energy Society, 37.
Hovel, H. J. (1978), *IBM J. Rev. Develop.*, Vol. 22, 112.
Hu, C., and Drowley, C. (1978), Record, 13th IEEE Photovoltaic Spec. Conf., 786.
James, L. W., and Williams, J. K. (1978), Record, 13th IEEE Photovoltaic Spec. Conf., 673.

Kaminar, N., Borden, P., Gregory, P., Grovner, M., and LaRoue, R. (1982), 16th IEEE Photovoltaic Spec. Conf. (to be published).
Ludman, J. E. (1982), *Applied Optics*, Vol. 21, 3057.
Maycock, D. D. (1978), Record, 13th IEEE Photovoltaic Spec. Conf., 5.
Meinel, A. B., and Meinel M. P. (1976), *Applied Solar Energy*, Addison-Wesley.
O'Donnell, D. T. et al. (1978), Record, 13th IEEE Photovoltaic Spec. Conf., 804.
Rapp, C. F., and Boling, N. L. (1978), Record, 13th IEEE Photovoltaic Spec. Conf., 690.
Swedlow (1976), Report No. 873, Swedlow, Inc., Garden Grove, Calif.
Welford, W. T., and Winston, R. (1978), *The Optics of Nonimaging Concentrators: Light and Solar Energy*, Academic Press.
Winston, R. (1974), *Solar Energy*, Vol. 16, No. 2, 89.

PROBLEMS

5.1 *Compound parabolic (Winston) concentrator* Show with words and a drawing that incident light beams within the acceptance angle of the compound parabolic concentrator reach the solar cell after at most one reflection.

5.3 *Energy cost as function of cell cost* Using Eq. (5.2.1), calculate the cost/kWh as function of the cost per m^2 of cells.

5.3 *Calculation of energy costs* Redo the calculations that result in Table 5.1, using your own estimates for the plant cost and other relevant figures or assume \$20/m^2 for a flat-plate system for land, support structure, etc., and \$100/m^2 for a concentrator system for land, concentrator, tracking structure, etc. Discuss how these changes impact the conclusions indicated in the text following Table 5.1.

5.4 *Effect of series resistance*

(*a*) Plot the *I-V* characteristics of a typical 10-cm^2 Si solar cell at 200× sun similar to Fig. 3.15*a*. Show the current and voltage scales.

(*b*) Draw the equivalent circuit of the cell including some internal series resistance R_s.

(*c*) In the plot of (*a*), add two more curves for $R_s = 0.01\ \Omega$ and $R_s = 0.05$. Graphically estimate the cell efficiency at $R_s = 0$, 0.01 Ω, and 0.05 Ω.

5.5 *Passive cooling* Explain with drawings and words why passive cooling can be effective for fresnel-lens concentrator systems regardless of the concentration ratio and why it would *not* be attractive for parabolic-trough concentrator systems.

CHAPTER

SIX

POWER CONDITIONING, ENERGY STORAGE, AND GRID CONNECTION

CHAPTER OUTLINE

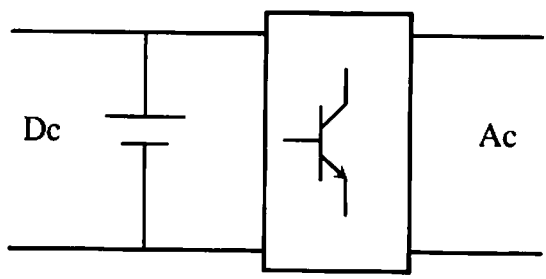

The electricity generated by a solar cell array is often processed electronically before it is fed to the load. The collective name for all the processing that may be performed is *power conditioning*. There may be some simple circuitry for protecting the array and the load from overvoltage and overcurrent. In the case of a battery load, a circuit that prevents overcharging and thus damaging the batteries is often employed. Only two major power-conditioning functions warrant discussion here. They are dc-to-ac inversion, and maximum-power-point tracking.

Dc-to-ac inversion is performed by an *inverter* that transforms the dc power generated by the solar cell array into ac power. This process is obviously necessary if the load, such as a group of electrical appliances, requires ac power. A farther-reaching reason for dc-to-ac conversion is to connect a solar cell array with the utility power grid, either at a central photovoltaic generation station or at a single-family residence with a rooftop solar cell array. Such a connection is highly attractive if the utility power grid is available. It solves two major problems of photovoltaic power generation—a guaranteed supply of power at all times and the storage of excess energy generated.

Whether the load requires ac or dc power, it is desirable to operate the solar cell array at its maximum power point (see Fig. 3.15) at all times. The array *I-V* characteristics change with light intensity and temperature, and the load in general changes unpredictably with time (due to load equipment's being turned on and off). What is desirable is a circuit that electronically and automatically matches the load with the array, in other words a maximum-power-point tracker.

Since photovoltaic power generation is intermittent in nature, some means of energy storage or power back-up is usually necessary. For stand-alone systems such as those located at remote sites, battery storage and/or a back-up diesel generator are commonly employed.

When the utility power is available as the back-up, as is the case in most regions of industrialized countries, an alternative to the expensive battery storage exists. The excess power generated by the solar cell array may be sold to and fed into the utility power grid. Such an integration with the power grid is natural for photovoltaic central generation stations, and it is economically attractive for small, residence-based systems, too. In a sense, the utility grid serves as the storage medium for the photovoltaic power in this scheme.

This brief introduction is summarized in Fig. 6.1. The simplest solar cell systems would involve none of the boxed items. Other systems could involve all of the boxed items.

6.1 MAXIMUM-POWER-POINT TRACKING

A solar cell array consists of many solar cells connected in a series/parallel fashion. The array has *I-V* characteristics similar to those of a single solar cell

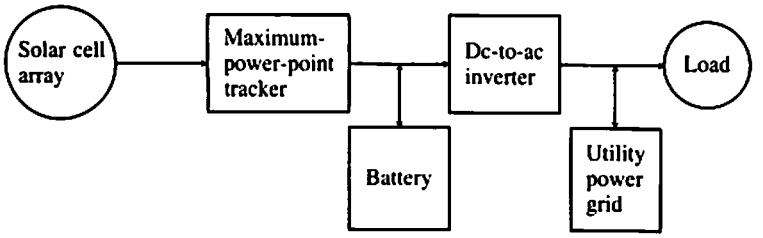

Figure 6.1 Block diagram illustrating power conditioning, energy storage, and integration with power grid. A given system may have all, some, or none of the four boxed items. The arrows denote the directions of power flows.

(Fig. 6.2). The *I-V* characteristics change in response to the variations in insolation. Each *I-V* curve has a maximum-power point (see Sec. 3.7), at which the product of the array voltage and current is maximized. It is clearly advantageous always to operate the array at its maximum-power point, hence the desire for maximum-power-point tracking.

Maximum-power-point tracking is not always employed nor is it always cost-effective. Consider a common type of load, the constant-voltage load such as a battery (or a connection to the utility grid through an inverter, to be discussed in Sec. 6.4). In Fig. 6.2 a battery voltage is chosen such that the array operates at its maximum-power point at noon on a clear day. At other times of the day or when the sky is not clear, the chosen battery voltage would cause the array to deliver less, but not far less, than the maximum possible power. This observation raises the question of whether the increased energy output can justify the cost of a maximum-power-point tracker.

An exact analysis of the benefit of tracking would be difficult because the maximum-power point also varies as a result of temperature changes and,

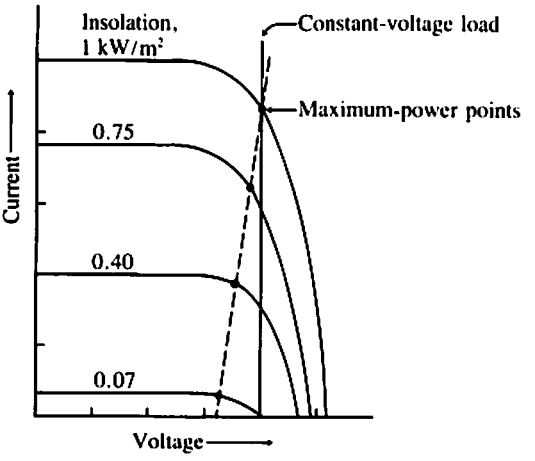

Figure 6.2 Typical *I-V* characteristics of a solar cell array. The maximum-power points vary with insolation as well as with temperature. A constant-voltage load such as a battery cannot extract the maximum power under all conditions.

possibly, aging of the array. Further, a battery is not an ideal constant voltage load. Its terminal voltage can vary by 30 percent depending on the state of charge and the charging or discharging current. Consequently, a maximum-power-point tracker may boost the annual energy output by 5 to 20 percent depending on the overall design and location of the solar cell system and the efficiency of the tracker.

At the present, smaller systems having battery storage do not employ maximum-power-point tracking. Even many of the very large demonstration systems were designed without tracking. In the future, maximum-power-point tracking will likely be attractive for solar cell systems connected to the utility power grid because the inverter should be able to perform the maximum-power-point tracking function at a small additional cost.

6.2 PRINCIPLES OF MAXIMUM-POWER-POINT TRACKERS

Assuming that the maximum-power point is at a lower voltage than the voltage of the battery load, what can be done about the mismatch? Obviously a dc "transformer" is needed. The function of dc voltage transformation is performed by a group of circuits known as *choppers*, or dc-to-dc converters.

Figure 6.3 shows one such circuit. The transistor operates in the *switch-*

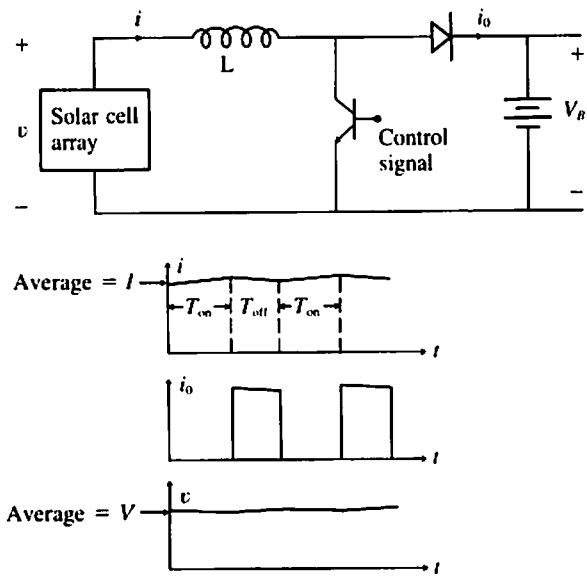

Figure 6.3 A maximum-power-point tracking circuit. By changing the ratio T_{on}/T_{off} the array may operate at any voltage below the battery voltage V_B.

ing mode. It is either off (open-circuit) or operating in the saturation region approximating a short circuit (with at most a few volts of voltage drop). When the transistor is on, the diode is reverse-biased and nonconducting and the array current flows through the inductor and the transistor. During this period, the current increases and so does the energy stored in the inductor, $\frac{1}{2}Li^2$. When the transistor is turned off, the array current flows through the inductor, the diode, and into the battery. During this period the difference between v and V_B (V_B shall be shown to be larger than v) causes a decrease in the inductor current. The goal, of course, is to set the average array current I at the maximum-power point. As i fluctuates around I on the array I-V curve, the array output voltage fluctuates around the maximum-power-point voltage, V.

Over one period, the array output energy must be equal to the energy delivered to the battery. Neglecting power losses in the inductor, transistor, and diode,

$$V \cdot I \cdot (T_{on} + T_{off}) = V_B \cdot I \cdot T_{off} \tag{6.2.1}$$

Canceling I from both sides,

$$V = \frac{T_{off}}{T_{on} + T_{off}} V_B \tag{6.2.2}$$

Therefore, the array can be made to operate at any voltage below the battery voltage V_B simply by adjusting the ratio T_{on}/T_{off}.

How do we determine when V and I have been set at the maximum-power point? Probably the simplest method is to recognize that at the maximum-power point the derivative of power ($v \cdot i$) with respect to v or i is equal to zero.

$$\frac{d(vi)}{dv} = v\frac{di}{dv} + i = 0 \tag{6.2.3}$$

$$\therefore \frac{di}{dv} = -\frac{i}{v} \approx -\frac{I}{V} \tag{6.2.4}$$

Since v and i continually fluctuate (see Fig. 6.3), the derivative di/dv can be evaluated every cycle and compared to I/V. When they are equal, the maximum-power point has been found [Eq. (6.2.4)]. If di/dv is larger than $-I/V$, then V is larger than the maximum-power-point voltage and must be lowered by increasing the ratio T_{on}/T_{off} (Landsman, 1978), and vice versa.

To avoid excessive deviations from the maximum-power point, the fluctuations in i and v must be limited by using a large inductance and/or a small $T_{on} + T_{off}$ period. Transistors are available up to 100 A and 500 V. For higher power capability, one can use thyristors, also known as SCRs (for silicon controlled rectifiers).

There are several chopper circuit configurations (Westinghouse, 1979 and Dewan, 1975). The circuit shown in Fig. 6.3 allows the array to operate

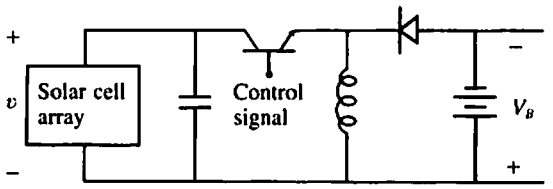

Figure 6.4 A maximum-power-point tracking circuit that allows the array to operate above and below V_B. $V = V_B T_{off}/T_{on}$. Note the reversal of the output polarity.

at voltages below V_B. A circuit that allows the array to operate above as well as below V_B is shown in Fig. 6.4. Chopper circuits are manufactured for electric cars and forklift trucks, however the control circuit for tracking the maximum-power point is not readily available yet.

6.3 STAND-ALONE INVERTERS

At a remote village or an energy self-sufficient house not connected to the utility power grid, there may still be a need for a dc-to-ac inverter because electrical appliances in general require ac power. In this case the circuit shown in Fig. 6.5 may be employed.

A clock alternately turns on T_1/T_4 and T_2/T_3 at 50 or 60 Hz frequency. The diodes are needed because the load may be reactive and the load current out of phase with voltage. When v_o is positive (T_1 and T_4 on), i_o may be negative (flowing through the two diodes in parallel with T_1 and T_4).

Although the 180° pulse waveform is simple to generate, it also contains significant amounts of third and fifth harmonics. The 120° pulse waveform contains less harmonics. In particular, it contains no third harmonics. Pulse-width-modulation techniques can further reduce the low-order harmonics.

The circuit can generate three-phase ac power if a third leg of transistors and diodes is added. There are many other types of inverters (Dewan, 1975; Westinghouse, 1979). Such free-standing inverters are the basis of commercial UPS (uninterruptible power supplies), which generate emergency ac power for critical equipment such as computers.

6.4 INVERTERS FUNCTIONING WITH POWER GRID

A utility power grid is an ac busbar of immense magnitude. One grid interconnects all the generation plants and users in a region of a country, in an entire country, or even across national boundaries. The grid is a rather rigid ac voltage source. Tens or hundreds of rotating generators on a grid operate at the same frequency and voltage because each generator is *locked* into the precise speed of rotation and voltage by the frequency and voltage of the grid.

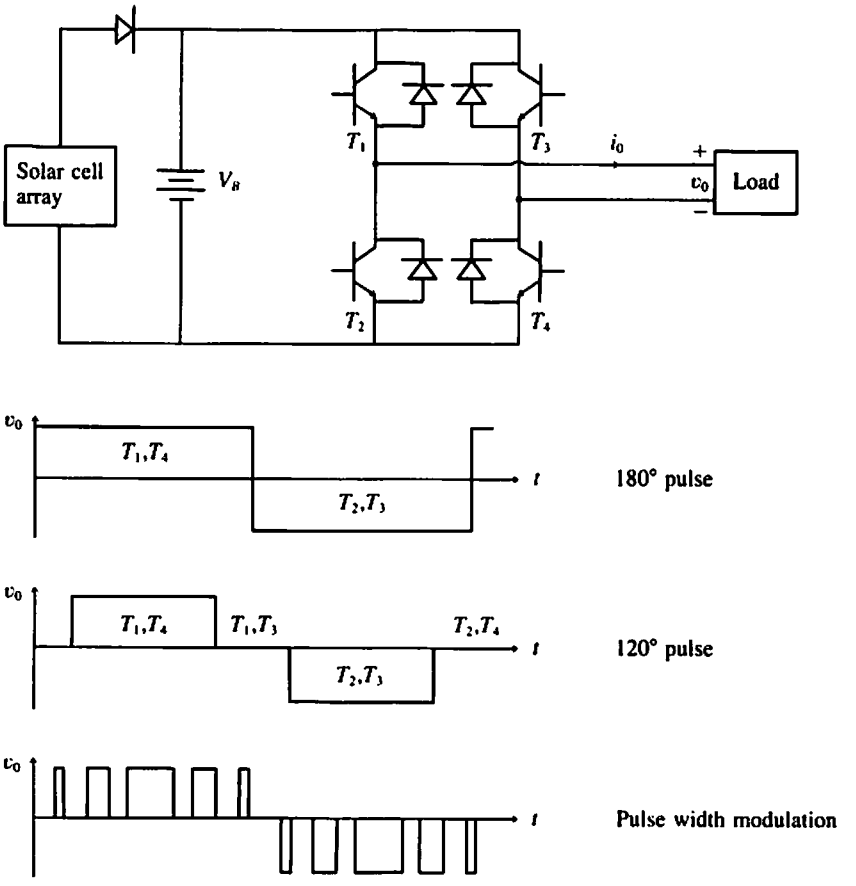

Figure 6.5 A single-phase inverter.

In a similar way, the presence of the power grid simplifies rather than complicates the inverter circuits.

Figure 6.6 shows an inverter that operates into a power grid. Some readers may recognize this circuit as a standard controlled rectifier—the kind widely used for controlling dc motors. Indeed, only the control circuitry of a controlled rectifier needs to be modified before it can be used as an inverter. When operated as an inverter it is called a *synchronous* inverter or a *line-commutated* inverter.

The four identical circuit elements are four thyristors. A thyristor is turned on by applying a short pulse to its gate (corresponding to the base of a transistor). Once turned on it can conduct current in the forward direction like a diode and stays on until the current flowing through it, for any reason,

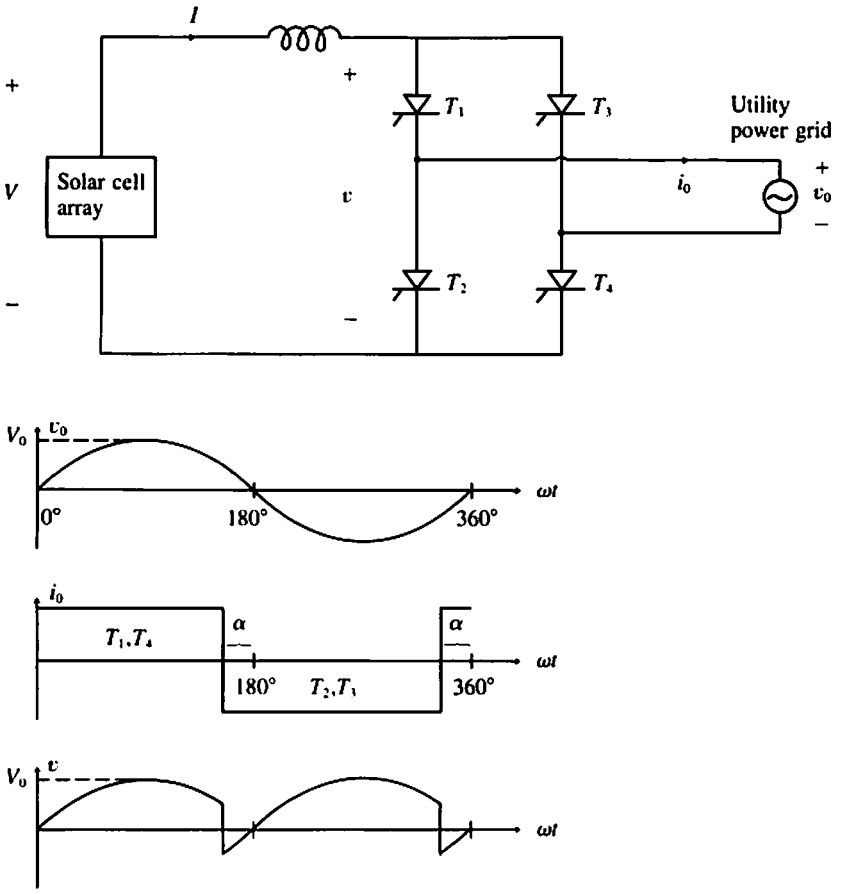

Figure 6.6 An inverter that connects the solar cell array with the utility power grid. The array operating voltage V may be adjusted by changing α.

drops to zero. At that moment it returns to the off state. The thyristors in Fig. 6.6 can only conduct currents in the downward direction.

Assume that the inductance is large enough so that an essentially constant current I flows through the array and the inductor. A control circuit senses the zero crossing of v_o, and turns on T_2 and T_3 $180 - \alpha$ degrees later ($|\alpha| < 90°$). So long as T_2 and T_3 remain on, i_o is negative regardless of the polarity of v_o. At $\omega t = 360° - \alpha$, T_1 and T_4 are turned on. The polarity of v_o is negative at that time, driving a current through the short circuit formed by T_4 and T_2 (also T_3 and T_1), in such directions as to turn T_2 (T_3) off. In the next half cycle, i_o is positive. Since α is less than 90° and probably close to 0°, i_o is nearly in phase with v_o. Thus power is being fed into the grid from the solar cell array.